[redacted]

Defense Documentation Center

Defense Supply Agency

Cameron Station • Alexandria, Virginia

[redacted]

Memo 221

Ref page for NRL MEMO Rept 221 dtd.

[redacted]

1) "Quantitative Measurements of Radar Echoes from Aircraft, I. B-36, B-45, F-51, and F-86," NRL Letter Report, Serial C-3460-73A/50 dated 24 October 1950.

2) "Quantitative Measurements of Radar Echoes from Aircraft, II. Formation of three F-86's, B-29, F-80 with wing tanks, and F-80 without wing tanks," NRL Letter Report, Serial C-3460-18A/51 dated 12 Feb. 1951.

3) "Quantitative Measurements of Radar Echoes from Aircraft, III. B-36 Amplitude Distributions and Aspect Dependence," NRL Letter Report, Serial C-3460-94A/51 dated 19 June 1951.

4) "Quantitative Measurements of Radar Echoes from Aircraft, IV. F-86 Amplitude Distributions and Aspect Dependence," NRL Letter Report, Serial C-3460-138A/51 dated 5 September 1951.

5) "Quantitative Measurements of Radar Echoes from Aircraft, V. Correction of X-band Values," NRL Letter Report, Serial C-3460-132A/52 dated [illegible] October 1952.

6. "Quantitative Measurements of Radar Echoes from Aircraft, VI. Corrected F-86 Amplitude Distributions and Aspect Dependence," NRL Letter Report, Serial C-3460-143A/52 dated 15 December 1952.

7) "Quantitative Measurements of Radar Echoes from Aircraft, VII. B-36 and F-86 Spectrums," NRL Memorandum Report No. 107 dated 15 January 1953.

8) "Quantitative Measurements of Radar Echoes from Aircraft, VIII. B-45," NRL Memorandum Report No. 116 dated 28 January 1953.

9) "Quantitative Measurements of Radar Echoes from Aircraft, IX. F-51," NRL Memorandum Report No. 127 dated 4 March 1953.

10) "Quantitative Measurements of Radar Echoes from Aircraft, X. Three F-86 Aircraft in Formation," NRL Memorandum Report No. 144 dated 6 April 1953.

11) "Quantitative Measurements of Radar Echoes from Aircraft, XI. B-29," NRL Memorandum Report No. 164 dated 25 May 1953.

[redacted]

[redacted]

NRL Memorandum Report 221

QUANTITATIVE MEASUREMENTS OF RADAR ECHOES FROM AIRCRAFT
XII. F-80

W. S. Ament
F. C. MacDonald
H. J. Passerini

RADIO DIVISION I

19 October 1953

NAVAL RESEARCH LABORATORY
Washington, D.C.

[redacted]

[redacted]

SECURITY

This document contains information affecting the national defense of the United States within the meaning of the Espionage Laws, Title 18, U.S.C., Sections 793 and 794. The transmission or the revelation of its contents in any manner to an unauthorized person is prohibited by law.

Further distribution of this report, or of an abstract, or reproduction may be made only with the approval of the Classified Material Control Officer, Naval Research Laboratory, Washington 25, D. C.

[redacted]

[redacted]

6

QUANTITATIVE MEASUREMENTS OF RADAR ECHOES
FROM AIRCRAFT.

XII. F-80.

9 Memorandum rept.,

By

10 W. S. Ament,
F. C. MacDonald
H. J. Passerini

11 19 Oct[redacted]53 12 58p.

~~Wave Propagation Research Branch~~
~~Radio Division I~~
Naval Research Laboratory
Washington 25, D. C.

(251950)

[redacted]

14 NRL-MR-221

mb

3

[redacted]

DISTRIBUTION

ANAF/GM Mailing List	43
CNO	
Attn: Op-03D	1
Attn: Op-05	1
Attn: Op-42	1
Attn: Op-342E	1
Attn: Op-374	1
ONR	
Attn: Code 427	1
Attn: Code 459	1
Attn: Code 470	1
BuAer	
Attn: El 80	1
BuOrd	
Attn: Re4f	1
BuShips	
Attn: Code 801	1
Attn: Code 820	1
Attn: Code 835	1
ComOpDevFor	1
WSEG	2
CO and Dir., USNEL	2
OCSigO	
Attn: Ch., Eng. and Tech. Div. SIGTM-S	1
CO, SCEL	
Attn: Dir. of Eng.	2
CO, Rome Air Dev. Center - Griffis A.F.B., Rome, N. Y.	
Attn: ENR	1
CO, Air Force Cambridge Research Labs	
Attn: ERRS	1

[redacted]

Dir., NBS Attn: CRPL	1
Office, Asst. Sec. of Defense (R and D) Attn: Information Requirements Branch	2
Attn: Navy Secretary	1
Attn: Committee on Electronics (Secretariat) For further distribution to: Advisory Group on Antenna and Propagation, and Subpanel on Radar Reflection Characteristics	30
BJSM (Navy Staff)	1
BJSM (Army Staff)	1
BJSM (Air Staff)	1
Canadian Joint Staff Attn: Navy Member	5
Australian Joint Service Staff	5
ASRE, England	1
DRE, Admiralty, England	1
Ministry of Supply, England	1
RRDE, England	1
TRE, England	1

~~CONFIDENTIAL~~

ABSTRACT

The characteristics of X-, S-, and L-band radar echoes from F-80 aircraft, with and without wing tanks, are presented in this report. Amplitude distributions of ten-second samples of the F-80 echo show that the general range of echo fluctuation is somewhat less than that found in propeller-driven aircraft or in large jet aircraft. The relative fluctuation of the echo is least near broadside, where the large echo component arising from the fuselage dominates the total echo. No clearly discernible effect of the wing tanks is found in the amplitude distributions, presumably owing to the small radar area of the wing tanks.

At certain aspects, however, the wing tanks apparently caused a distinct modulation in the echoes at rates proportional to radar frequency. Aside from such modulations, the fluctuations of the F-80 echo had continuous low-frequency spectrums of width proportional to radar frequency.

For the aspects measured, the average median radar area outside of the broadside region is roughly independent of frequency and is equal to about 1 square meter. For the broadside region, which has a two-humped shape, the average median radar area is equal to 20 square meters. Presence of wing tanks did not affect the average S-band median radar area appreciably.

~~CONFIDENTIAL~~

CONFIDENTIAL

PROBLEM STATUS

This is an interim report on the problem; work continues.

AUTHORIZATION

NRL Problem R11-17
WADC CSO No. 52-849

CONFIDENTIAL

Introduction

In eleven previous reports,(1)-(11) characteristics of radar echoes from various aircraft were given. This report, the twelfth of the series, gives the complete results obtained for the F-80, with and without wing tanks. The measurements on the F-80 were taken during three days of operation, but absolute X-band results were deducible for only the final day's runs, owing to calibration difficulties on the earlier days.

Amplitude Distributions

The amplitude distributions plotted in Figs. 2-6 are representative ten-second (1200-pulse) samples of the encountered airplane aspects (defined in Fig. 1). In these Figures, cumulative distributions of echo pulse amplitudes are plotted, the ordinate being $10 \log_{10} \sigma$ (σ = radar area in square meters), and the abscissa, the percent of time the amplitude of the observed echo exceeds the ordinate. For comparison, a straight line is drawn with the same slope as the theoretical cumulative distribution (Rayleigh distribution) of noise powers.

On the various plots, points indicated by ⊡, ⊙ and △, represent X-, S-, and L-band observations, respectively. Thus, distributions plotted against a single ordinate scale represent simultaneous observations, at two different radar frequencies, of the distribution of radar areas, the intention being to emphasize <u>differences</u> between the radar area distributions. Again for purposes of comparison, at the top and bottom of each figure are

distributions pertaining to the F-80 with and without wing tanks, respectively, for roughly the same aspect angles.

In the main, the amplitude distributions can be fitted well with straight lines corresponding to the theoretical Rayleigh distribution. Where the echo from the fuselage is strong, namely at azimuths 80° - 100° (Fig. 4), there is some tendency for the best-fitting straight lines to be more nearly horizontal than the theoretical Rayleigh lines. Generally speaking, this tendency is most marked for the L-band distributions. This can be explained in the following way:

The Rayleigh distribution is that expected if the echo were composed of a large number of component echoes having a large variety of relative phases during the period of echo measurement. The fact that the F-80 echo is approximately Rayleigh distributed (i.e., well fitted with the theoretical Rayleigh line) implies that there are several 'bright points', or strongly echoing parts of the F-80 surface at the observed aspects, and, furthermore, that the relative phases of the echoes from the several bright points are changed through several radians as the aircraft's aspect changes during the ten seconds of observation. As the rate of phase variation is proportional to the radar frequency, other things being equal, the L-band echo components would have the least relative phase variation, and hence the L-band echo should be the steadiest among the three frequencies used. This serves to explain the occasionally relatively steady L-band echoes, indicated in the

plots (e.g. Figs. 3 and 5) by an L-band distribution having a more gradual slope than the simultaneously observed S- and X-band distributions. The horizontal tendency at azimuth angles 86° - 93° (Fig. 4) seems attributable to the fact that the echo from the fuselage is by far the strongest component echo. According to plan drawings of the F-80, the fuselage is curved, so that its echo should persist with relatively constant magnitude throughout the sampled 7° of aspect, unless the wing should shadow the point of geometric reflection. Echoes from the remainder of the F-80 are apparently too weak to cause the usual degree of fluctuation through constructive and destructive interference with the dominant fuselage echo.

The presence of wing tanks appears to make little difference in the amplitude distributions, showing the relative smallness of the wing-tank echoes at the azimuths sampled. The wing tank creates one more "bright point" from which the echo phase varies relatively rapidly, owing to the physical distance of the wing tank from the fuselage, where the bulk of the bright points lie. Thus the addition of the wing tank should result in echoes more nearly Rayleigh distributed than those observed at the same aspect interval in the absence of the wing tanks. The average radar area (the ordinate at the 63rd percentile) is increased by the average radar area of the wing tank. Thus if, for a particular band of aspects, the radar area of the wing tank averages 25% of that of the rest of the F-80, the total F-80 radar area is increased by a factor 1.25, or about 1 db, an increase too small to detect

with any certainty. Under the same circumstances, however, the voltage amplitude of the wing tank echo is 50% of that from the rest of the aircraft, so that the echo fluctuations produced by the addition of the wing tank can be quite marked.

The theoretical radar echo from a jet aircraft is discussed in more quantitative detail in Report VIII, which deals with the radar properties of the B-45. Amplitude distributions of the B-45 echo were more nearly Rayleigh distributed than is the case with the F-80, owing to the more extended structure of the B-45 as a radar echoer; the jet pods of the F-80 are faired into the fuselage, while those of the larger B-45 are mounted on the wings.

Aspect Dependence

Each of Figs. 7-16 covers one flight of the aircraft, and consists of three graphs. The uppermost graph of each figure consists of a plot of the aircraft's aspect, as defined in Fig. 1, versus range in thousands of yards. Each graph consists of three sets of points, each set being connected by straight line segments. Each point represents about one second of data, and data taken simultaneously are aligned vertically so that the uppermost point in each graph is the maximum, the middle point is the median, and the lowest point is the minimum radar area occurring in that second. The radar area as plotted contains variations due to interference lobes caused by ground reflections. At the center of each lobe, or integral number of lobes, the symbol

(⊗) indicates the median value (reduced to "free-space" value in accordance with the procedure described in the Appendix to (2)) of the one-second median radar area values for that lobe or integral number of lobes, and these median values were used in determining the median value of σ for each five degrees of azimuth as described below.

At the bottom of each plot, the step-like curve gives the radar area, in 1 db increments, of a target just detectable by the radar at the particular range (neglecting the receiver recovery time characteristic). Therefore, the step-curve really represents minimum detectable area only at ranges beyond receiver recovery.

The data were divided into intervals, each of which spanned five degrees of azimuth. For each such interval the median of the one-second median points was determined for each frequency. These "median-median" values are plotted in Fig. 17 for the F-80 with wing tanks (Figs. 7-13) and Fig. 19 for the F-80 without wing tanks (Figs. 14-16).

The target azimuth, as calculated from the recorded azimuth of the optically pointed radar and the true heading assigned to the F-80 for the particular run, was not concordant with the azimuth determined from the positions of the echoes from the fuselage. The differences ranged from 5° to 20°. The azimuth angles, therefore, have been changed to agree with the expected positions of the fuselage echoes. Due to the absence of a broadside echo in Runs 7 and 11 for 3/1/50, the azimuth angles quoted in Figs. 22, 25,

28 and 33 were calculated from the recorded azimuths, and are therefore uncertain.

Both the azimuth correction and the nature of the F-80 echo near broadside aspect may be discussed with reference to the aircraft's structure, as revealed in plan drawings of the F-80. These drawings show that the forward portion of the fuselage may be fitted with a forward-pointing truncated cone of half-angle 7-3/4°, and the stern portions by a rearward-pointing truncated cone of half-angle 7-1/4°. The central portions of the fuselage are partially hidden from the radar by the wing. Thus the echo from the fuselage should rise rather sharply near azimuth 82° and peak again sharply near azimuth 97°, making the angular range of fuselage echo between peaks about 15°. In all F-80 runs providing aspects in this azimuth region, echoes attributable to the fuselage were found through azimuth bands of the anticipated angular width, but having a variety of nominal azimuths as calculated from assigned headings. Thus, as far as was possible, aspects listed in this report have been corrected to make the fuselage echoes maximum at listed azimuths 82° and 97° respectively.

Between the forward and aft conical sections, the fuselage of the F-80 tapers in a long curve, the central portions of which are partially hidden by the wing. With this structure, the fuselage would be expected to produce an echo independent of radar frequency over at least the range X to L band. A plot of fuselage echo versus azimuth thus should be a two-humped affair, the

relatively weak echo between the humps showing the shadowing effect of the wing. Such a plot should represent the total F-80 echo for these azimuths, if the echoes from the remainder of the airplane are relatively weak, as seems probable, even with the wing tanks. This reasoning serves to explain the similarities found among Figs. 7-16 over azimuths 78° through 102° for all cases where saturation effects or ground clutter do not eliminate the two-humped appearance of the broadside region echo. The two-humped feature of the azimuth dependance is clearly evident in Figs. 17-21.

On theoretical grounds, the wing tanks should not raise the average echo power level significantly. As a first approximation, the wing tank may be regarded as a 1/3 scale model of the fuselage, mounted parallel to the fuselage. For most aspects, one can calculate the radar area by the principles of physical optics. According to these principles, the radar area of the wing tank should always be $(1/3)^2$ the radar area of the geometrically similar, similarly oriented fuselage. Thus at all aspects, a single wing tank's echo power approximates 1/9 that of the rest of the F-80.

The aspect angles of the present measuring program always provided a clear line-of-sight view of both wing tanks (if the F-80 had been in level flight) and both must therefore be considered in discussing the radar echo. The wing tank is a tear-drop-shaped figure of revolution, mounted under the wing tip approximately tangent to the lower surface of the wing. Over the 7° azimuth interval 90° - 97° radar rays can be reflected by the under surface of the wing farthest from the radar, to strike the far wing tank at

normal incidence. Thus, in this narrow azimuth band, both the far wing tank and its mirror image in the under surface of the wing can produce radar echoes, which combine at the radar with relative phases determined by radar wavelength and the elevation angle. The total echo of the far tank and its image can be up to 16 times as powerful as the echo from the isolated wing tank, though this figure must be somewhat reduced owing to the slight positive curvatures of the wing surface. Ignoring this curvature, and averaging over elevation angles, gives an average echo power, for the far tank and its image, of four times that of the isolated wing tank, a figure applying in the azimuth interval 90° - 97° only. In other azimuth intervals, there is no mirror image of the far wing tank, and its echo power is about the same as that of the near wing tank. Thus the total echo power produced by the wing tanks averages twice the echo power of a single wing tank, except in the aspect interval 90° - 97° where the average may be five times that of the single wing tank. It seems reasonable to estimate that the echo power contributed by both wing tanks, averaged over all aspects, is about three times the average echo power that would be produced by a single wing tank, viewed over all aspects. Thus the average power added to the F-80 echo by the wing tanks is estimated as 3/9 = 33% of the average echo power in the absence of wing tanks. This theoretical enhancement is about 1.2 db. In spite of the generous allowance for three tanks, the estimate may be somewhat low, owing to the fact that some of the stronger echoes from the fuselage are cut off by the wing. This

shadowing occurs in the azimuth interval 85° - 95°, as is most obvious in Fig. 21. In this figure, it will be noticed that the S-band radar area for the F-80 <u>without</u> wing tanks averages some 2-1/2 db <u>lower</u>, in the azimuth interval 85° - 95° than the S-band area for the tank-carrying F-80. In this aspect interval, then, the presence of the wing tanks <u>does</u> make a significant difference in the average radar area.

<u>Frequency Dependence</u>

To obtain representative measures of the radar area of the F-80, the following procedure was carried out for each radar frequency employed. From Fig. 17 for the F-80 with wing tanks and from Fig. 19 for the F-80 without wing tanks, a single number for the radar area was obtained on each frequency for each five-degree azimuth interval by averaging all the "median-median" areas (in square meters) in that azimuth interval, without regard to elevation angles involved. The results are plotted in Fig. 18 for the F-80 with wing tanks and in Fig. 20 for the F-80 without wing tanks, separate symbols being used for each frequency.

In order to arrive at a factor representing frequency dependence, the following procedure was used: The five-degree averages discussed above which contained data on <u>both</u> L and S bands (for the F-80 with tanks) were selected. The ratio of L-band area to S-band area was determined for each interval, and the average value for all the common intervals found. A similar procedure was carried out for the S- and X-band data (for the F-80

without wing tanks). Finally, the common five-degree intervals for which S-band data were available for the F-80 with and without wing tanks were processed in the same way. The average ratios found are given in the following table, together with the number of common five-degree intervals for which data were available:

	Ratio	No. of Intervals
(σ_L/σ_S) avg.	1.3	18
(σ_X/σ_S) avg.	1.4	8
$(\sigma_{tanks}/\sigma_{no\ tanks})$ avg.	1.5	11

In view of the limited number of common intervals, the conclusions which can be drawn are that the average radar area is roughly independent of frequency and that the presence of wing tanks makes a small difference, at most, in the average radar area.

Since the average radar area is found to be essentially independent of frequency, the data on all frequencies were used to find representative average values of radar area. For the region excluding the broadside region of strong echoes (i.e., outside the azimuth range 70° - 110°) the average radar area comes out to be 1.3 square meters. For the broadside region (70° - 110°), the average radar area is 20 square meters. The broadside region has a two-humped structure, as discussed previously, so that for greater detail Fig. 21 should be used.

Fluctuations of the F-80 Echo

Spectrums of selected five-second samples of F-80 echoes were

prepared according to the procedure described in Report VII. The necessary plots of video voltage versus time are shown in Figs. 22-27 and the spectrums for aspects near head-on, near broadside, and toward the tail are shown in Figs. 28-35. Following the method described in Report IX, the spectrums are also plotted against an expanded frequency scale.

The pulse-by-pulse voltage plots on each figure reproduce, from top to bottom, the L-, S-, and X-band echoes obtained from the F-80 at approximately one aspect and one general angular rate. Especially on Fig. 24, it is apparent that the same general average echo behavior is found on all three frequencies, with fluctuation rates, however, roughly proportional to radar frequency. Thus, in the spectrums of Figs. 31 and 32, the L- and S-band spectrums are roughly the same as the corresponding X-band spectrum (on a given figure) except for compressions of the frequency scale.

The F-80 structure is fairly compact, with only the thin wings (and the wing tanks) providing sources of radar echoes elsewhere than from the fuselage. In the plane of the wing, the echo from the wing proper is quite small, owing to the wing's sharply curved leading and trailing edges. The principal radar echoer well removed from the fuselage is the wing tank. The tear-drop shape of the wing tanks is such that its echo is maximum near broadside. The wing tank echo should taper from this maximum as the azimuth increases, and become almost negligible beyond azimuth 102°, since the half-angle of the conical stern of the wing tank is roughly 12° = 102° - 90°. At broadside the wing tank lies on the line of sight between the radar and the

fuselage. Hence the tank and the fuselage have about the same speed away from the radar, and the relative phase of their echoes does not vary rapidly. Thus the wing tank causes only slow echo fluctuations near broadside aspect, where its echo is strongest. At aspect 100° the wing tank echo is still reasonably strong, and it can beat reasonably rapidly with the echo from the after-portion of the fuselage, which should produce the major echo component. (The discussion of Report VIII gives the relevant theory for jet aircraft echo fluctuations in quantitative detail.)

The distinct frequencies visible on the S- and X-band voltage plots of Fig. 24 (109° - 112° azimuth) may well be caused by interference among the echoes from stern portions of the fuselage and the tapering aft portion of the two wing tanks. Along the course flown, the nominal angular rate of the F-80 relative to the radar was 0.6° or .01 radian per second. The separation of the after-cone of the F-80 and the nearer wing tank is about 25 feet, or 250 X-band wavelengths. Projected on a plane normal to the radar's line-of-sight, this separation is roughly 220 wavelengths, or 440 half-wavelengths. (The similar separation between the two wing tanks is about 400 wavelengths.) At the approximate angular rate of .01 radian/sec, the resulting X-band fluctuation frequency is (.01)x(440) = 4.4 cps, about that (4.3 cps) discernible on the X-band voltage plot of Fig. 24, and also in the corresponding spectrum at the bottom of Fig. 32. In the middle spectrum of this figure, the corresponding S-band frequency is found at 1.2 cps. This 1.2 cps

S-band fluctuation frequency is related to the corresponding observed X-band frequency 4.3 cps according to

$$\frac{1.2 \text{ cps}}{4.3 \text{ cps}} \approx \frac{\text{S-band radar frequency}}{\text{X-band radar frequency}} ,$$

showing that the two fluctuation frequencies arise from the phase differences between the same physical parts of the airplane.

Although the foregoing discussion is qualitatively correct, it is difficult to deduce quantitative information about the radar areas of various parts of the F-80 from either Fig. 24 or Fig. 32. One would have to explain why the intense modulations, observed in the voltage plots of Fig. 24, fade out at the right hand sides. (Corresponding to this fading, the spectrums of Fig. 31 "scintillate" at the respective modulation frequencies, owing to the finite response time of the spectrum analyzer.) Secondly, it is difficult to assign physical locations for strongly echoing surfaces of the F-80 at the listed azimuth, 112°. Thirdly, both wing tanks are visible to the radar when the F-80 is in level flight at the listed 5.3° - 5.5° elevation, and both probably give commensurable echoes. At the listed azimuth, the line of sight to the far wing tank passes under the aft section of the fuselage. The fadeout of the signal might possibly be explained by attributing a large part of it to the far wing tank and assuming that the F-80 dipped the near wing during the five seconds under consideration. If this wing dipped a mere 5°, it would cause the line of sight to the far wing tank to pass through the fuselage, thereby cutting off the echo from the far wing tank.

Thus, various combinations of one or two wing-tank echoes would have to be considered, depending particularly on the amount of roll which occurred during the flight. In the absence of such roll information, it is not possible to provide a complete detailed explanation of the observed spectrum characteristics.

Conclusions

The characteristics of X-, S-, and L-band radar echoes from F-80 aircraft, with and without wing tanks, are presented in this report. Amplitude distributions of ten-second samples of the F-80 echo show that the general range of echo flucutation is somewhat less than that found in propeller-driven aircraft or in large jet aircraft. The relative fluctuation of the echo is least near broadside, where the large echo component arising from the fuselage dominates the total echo. No clearly discernible effect of the wing tanks is found in the amplitude distributions, presumably owing to the small radar area of the wing tanks.

At certain aspects, however, the wing tanks apparently caused a distinct modulation in the echoes at rates proportional to radar frequency. Aside from such modulations, the fluctuations of the F-80 echo had continuous low-frequency spectrums of width proportional to radar frequency.

For the aspects measured, the average median radar area outside of the broadside region is roughly independent of frequency and is equal to about 1 square meter. For the broadside region, which has a two-humped

shape, the average median radar area is equal to 20 square meters. Presence of wing tanks did not affect the average S-band median radar area appreciably.

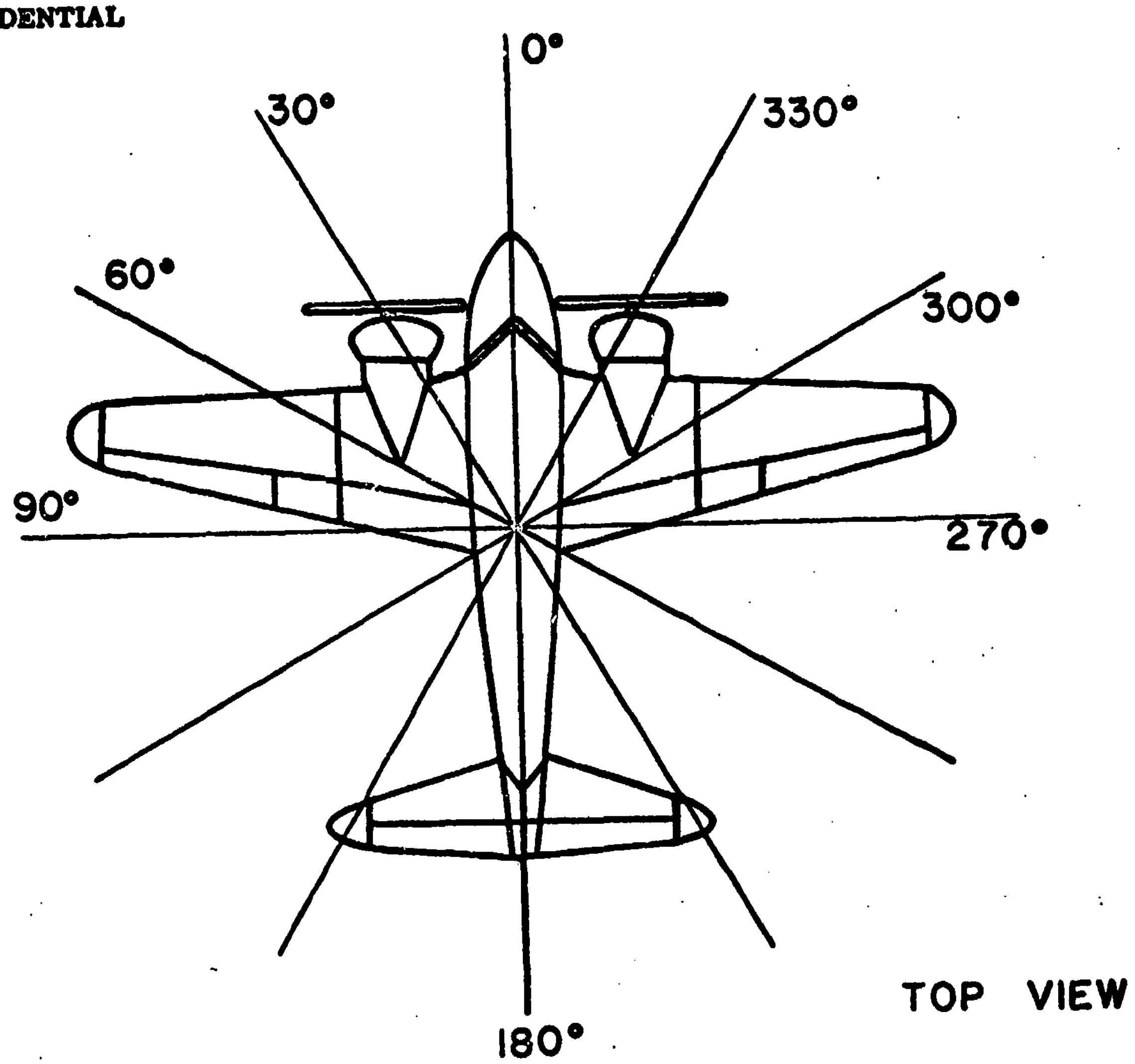

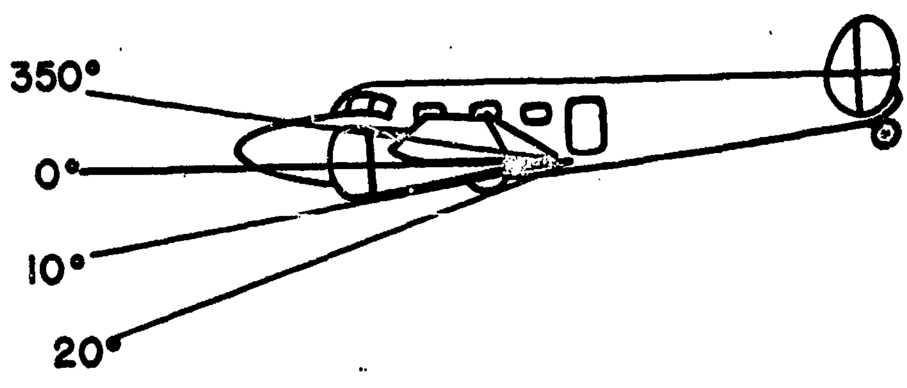

Definition of aspect angles

Figure 1

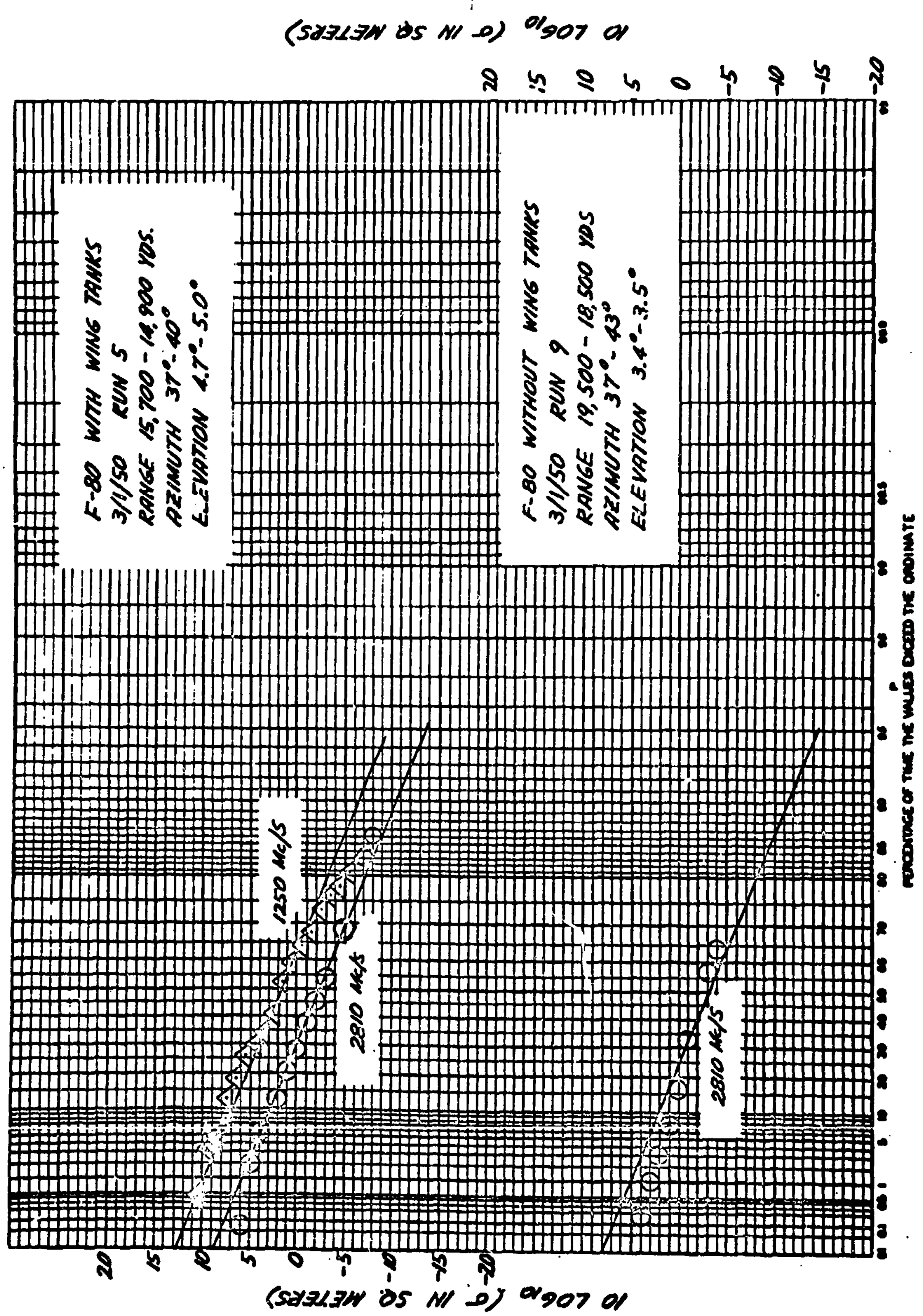
10 LOG10 (σ IN SQ METERS)
20 15 10 5 0 -5 -10 -15 -20
F-80 WITH WING TANKS
3/1/50 RUN 5
RANGE 15,700 - 14,900 YDS.
AZIMUTH 37°-40°
ELEVATION 4.7°-5.0°
F-80 WITHOUT WING TANKS
3/1/50 RUN 9
RANGE 19,500 - 18,500 YDS
AZIMUTH 37°-43°
ELEVATION 3.4°-3.5°
1250 Mc/S
2810 Mc/S
2810 Mc/S
PERCENTAGE OF TIME THE VALUES EXCEED THE ORDINATE
20 15 10 5 0 -5 -10 -15 -20
10 LOG10 (σ IN SQ METERS)

Figure 2

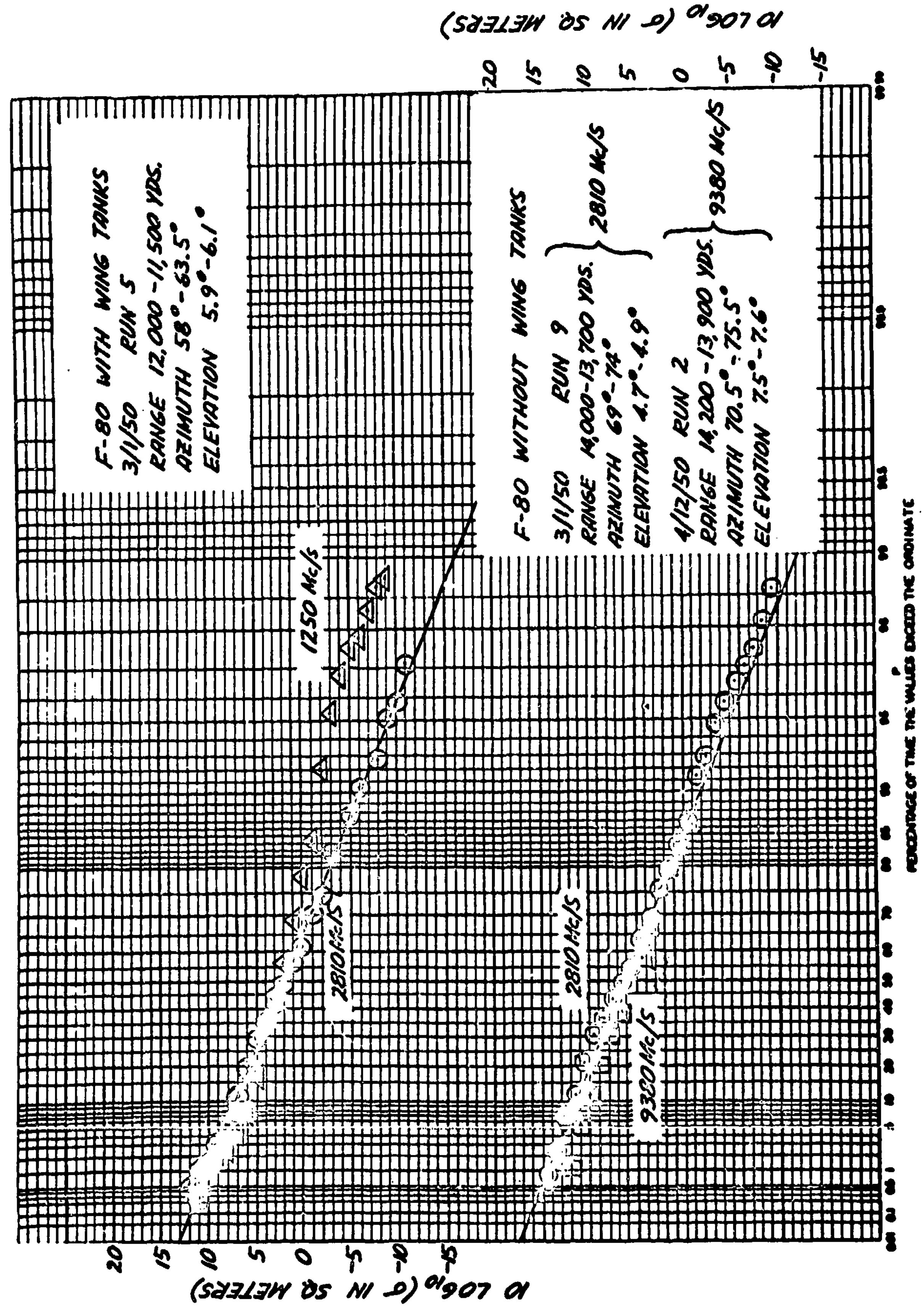

F-80 WITH WING TANKS
3/1/50 RUN 5
RANGE 12,000-11,500 YDS.
AZIMUTH 58°-63.5°
ELEVATION 5.9°-6.1°
F-80 WITHOUT WING TANKS
3/1/50 RUN 9
RANGE 14,000-13,700 YDS.
AZIMUTH 69°-74°
ELEVATION 4.7°-4.9°
2810 Mc/S
4/12/50 RUN 2
RANGE 14,200-13,900 YDS.
AZIMUTH 70.5°-75.5°
ELEVATION 7.5°-7.6°
9380 Mc/S
1250 Mc/S
2810 Mc/S
2810 Mc/S
9300 Mc/S
10 LOG10 (σ IN SQ METERS)
20 15 10 5 0 -5 -10 -15
PERCENTAGE OF TIME THE VALUES EXCEED THE ORDINATE

Figure 3

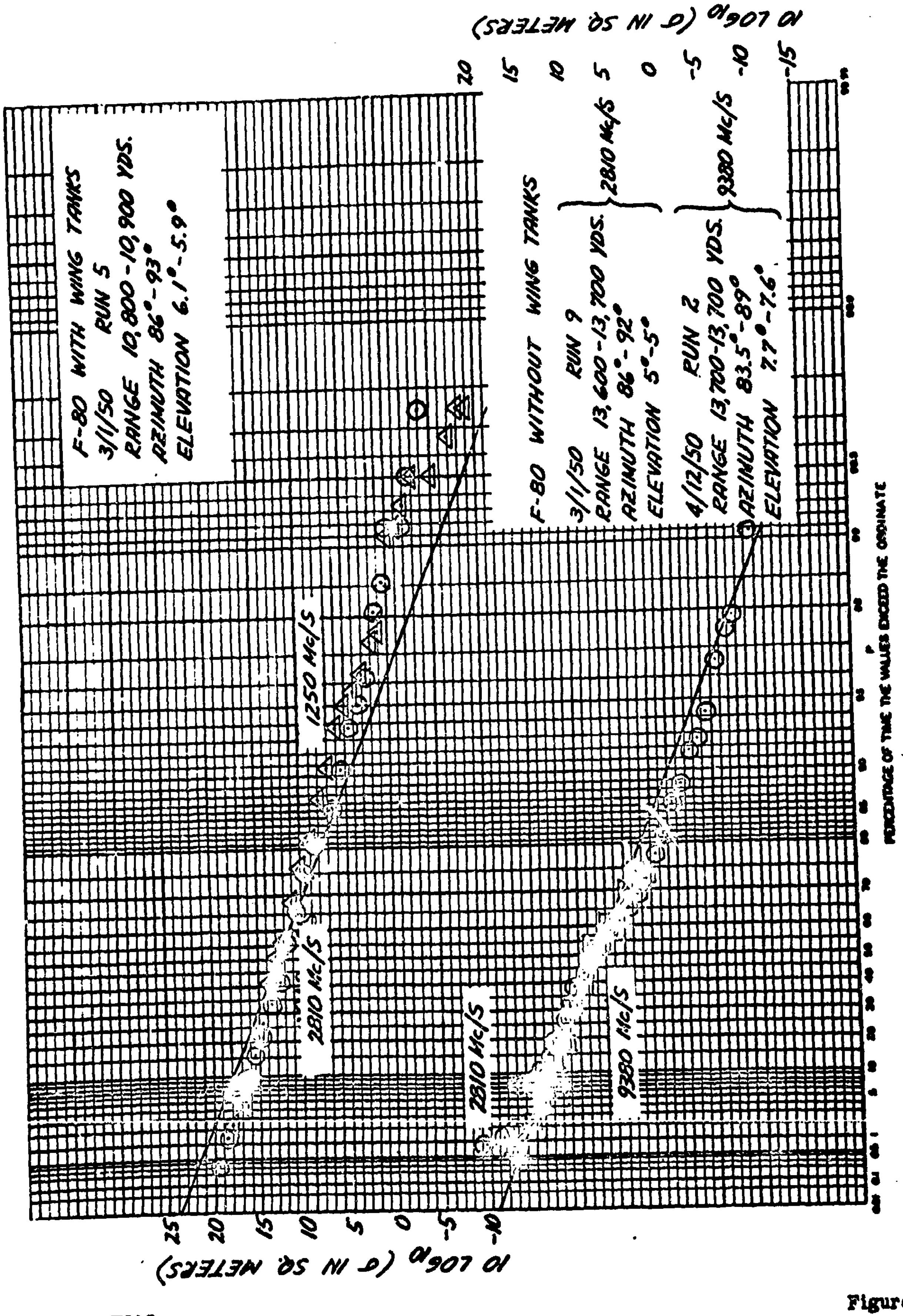

F-80 WITH WING TANKS
3/1/50 RUN 5
RANGE 10,800-10,900 YDS.
AZIMUTH 86°-93°
ELEVATION 6.1°-5.9°
F-80 WITHOUT WING TANKS
3/1/50 RUN 9
RANGE 13,600-13,700 YDS.
AZIMUTH 86°-92°
ELEVATION 5°-5°
2810 Mc/S
4/12/50 RUN 2
RANGE 13,700-13,700 YDS.
AZIMUTH 83.5°-89°
ELEVATION 7.7°-7.6°
9380 Mc/S
1250 Mc/S
2810 Mc/S
2810 Mc/S
9380 Mc/S
10 LOG10 (σ IN SQ. METERS)
25 20 15 10 5 0 -5 -10
20 15 10 5 0 -5 -10 -15
PERCENTAGE OF TIME THE VALUES EXCEED THE ORDINATE

Figure 4

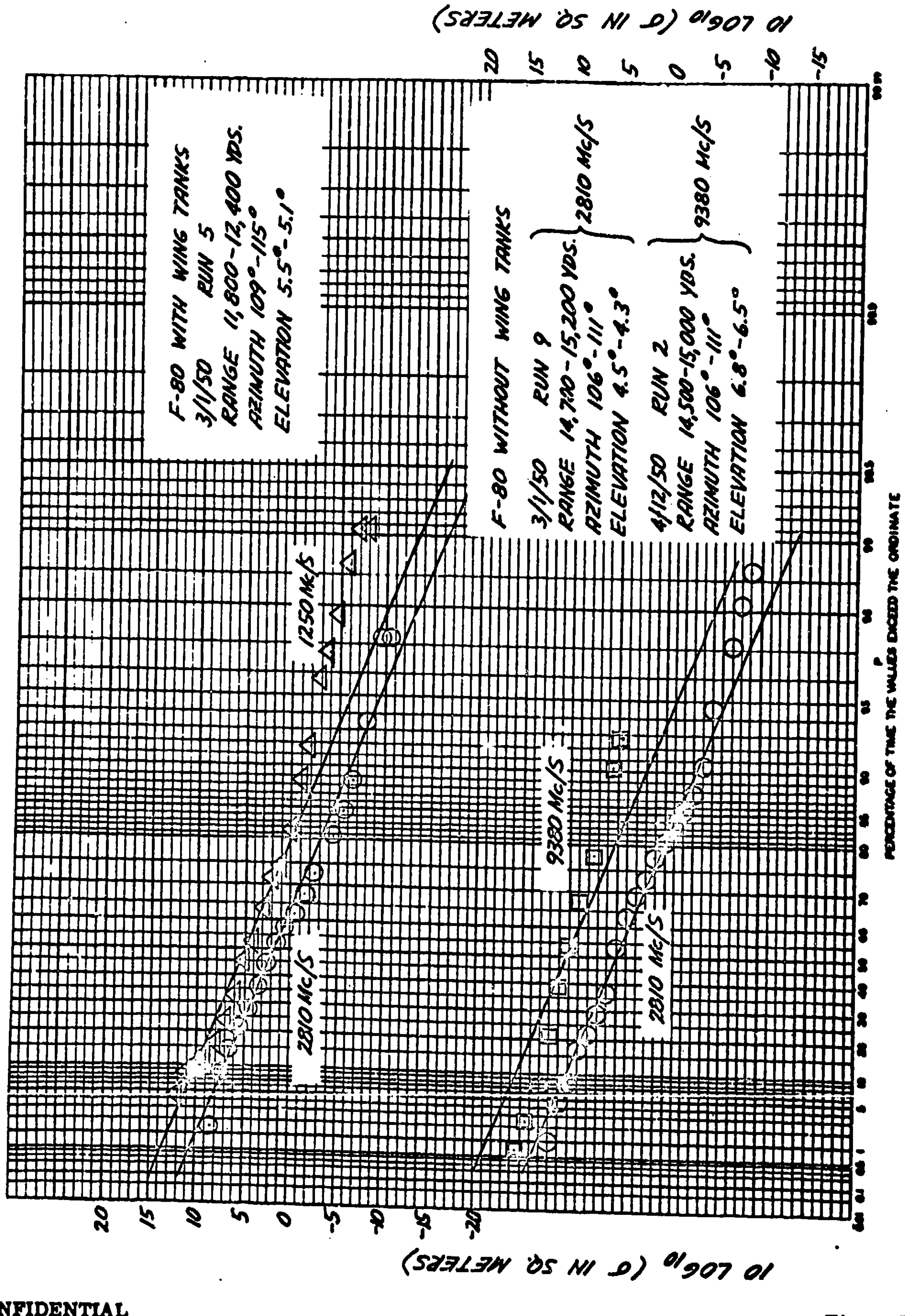

F-80 WITH WING TANKS
3/1/50 RUN 5
RANGE 11,800-12,400 YDS.
AZIMUTH 109°-115°
ELEVATION 5.5°-5.1°
F-80 WITHOUT WING TANKS
3/1/50 RUN 9
RANGE 14,700-15,200 YDS.
AZIMUTH 106°-111°
ELEVATION 4.5°-4.3°
2810 Mc/S
4/12/50 RUN 2
RANGE 14,500-15,000 YDS.
AZIMUTH 106°-111°
ELEVATION 6.8°-6.5°
9380 Mc/S
1250 Mc/S
2810 Mc/S
9380 Mc/S
2810 Mc/S
10 LOG10 (σ IN SQ. METERS)
20 15 10 5 0 -5 -10 -15 -20
PERCENTAGE OF TIME THE VALUES EXCEED THE ORDINATE

Figure 5

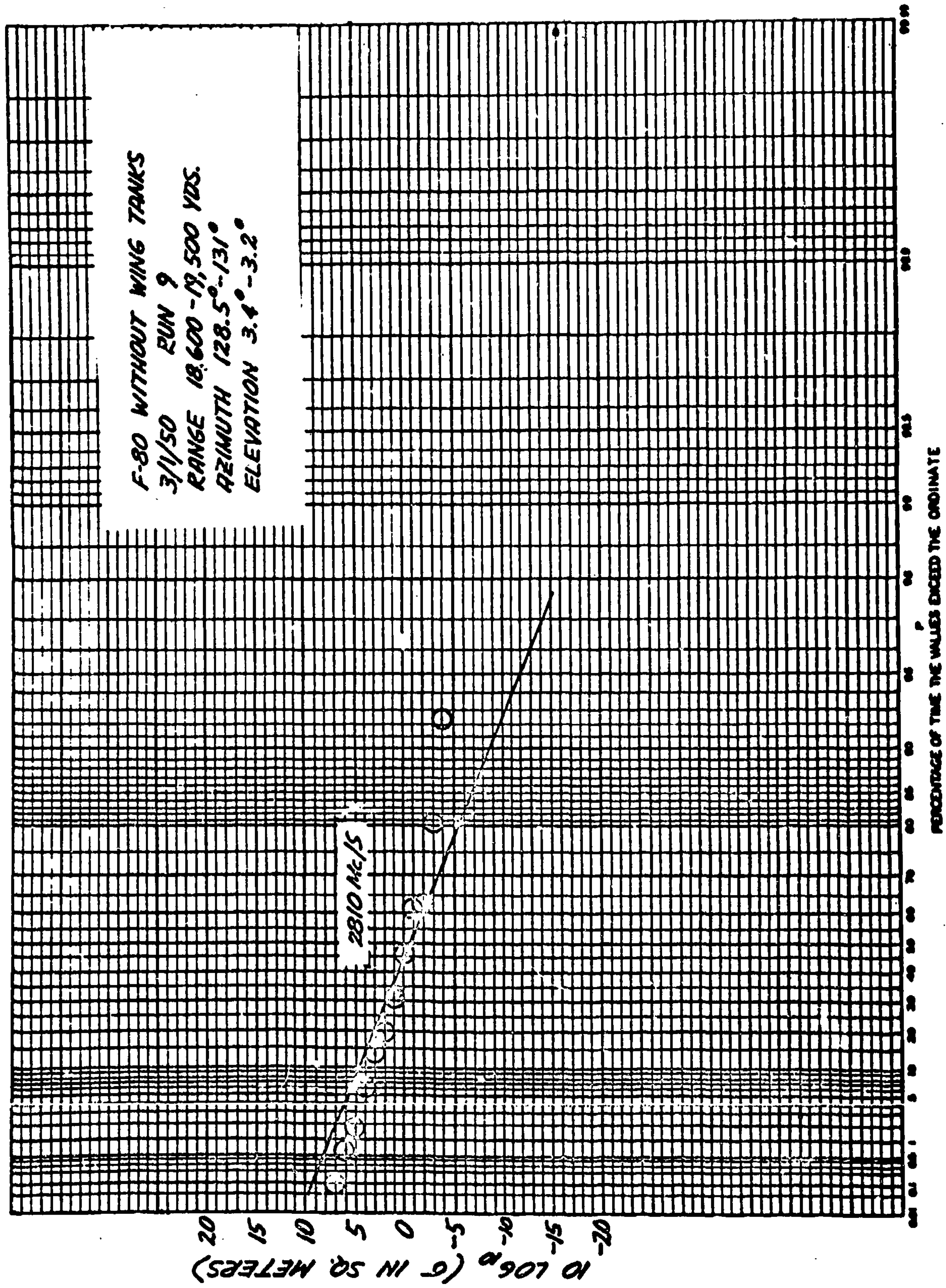
F-80 WITHOUT WING TANKS
3/1/50 RUN 9
RANGE 18,600-19,500 YDS.
AZIMUTH 128.5°-131°
ELEVATION 3.4°-3.2°
2810 Mc/S
20 15 10 5 0 -5 -10 -15 -20
10 LOG10 (σ IN SQ. METERS)
PERCENTAGE OF TIME THE VALUES EXCEED THE ORDINATE

Figure 6

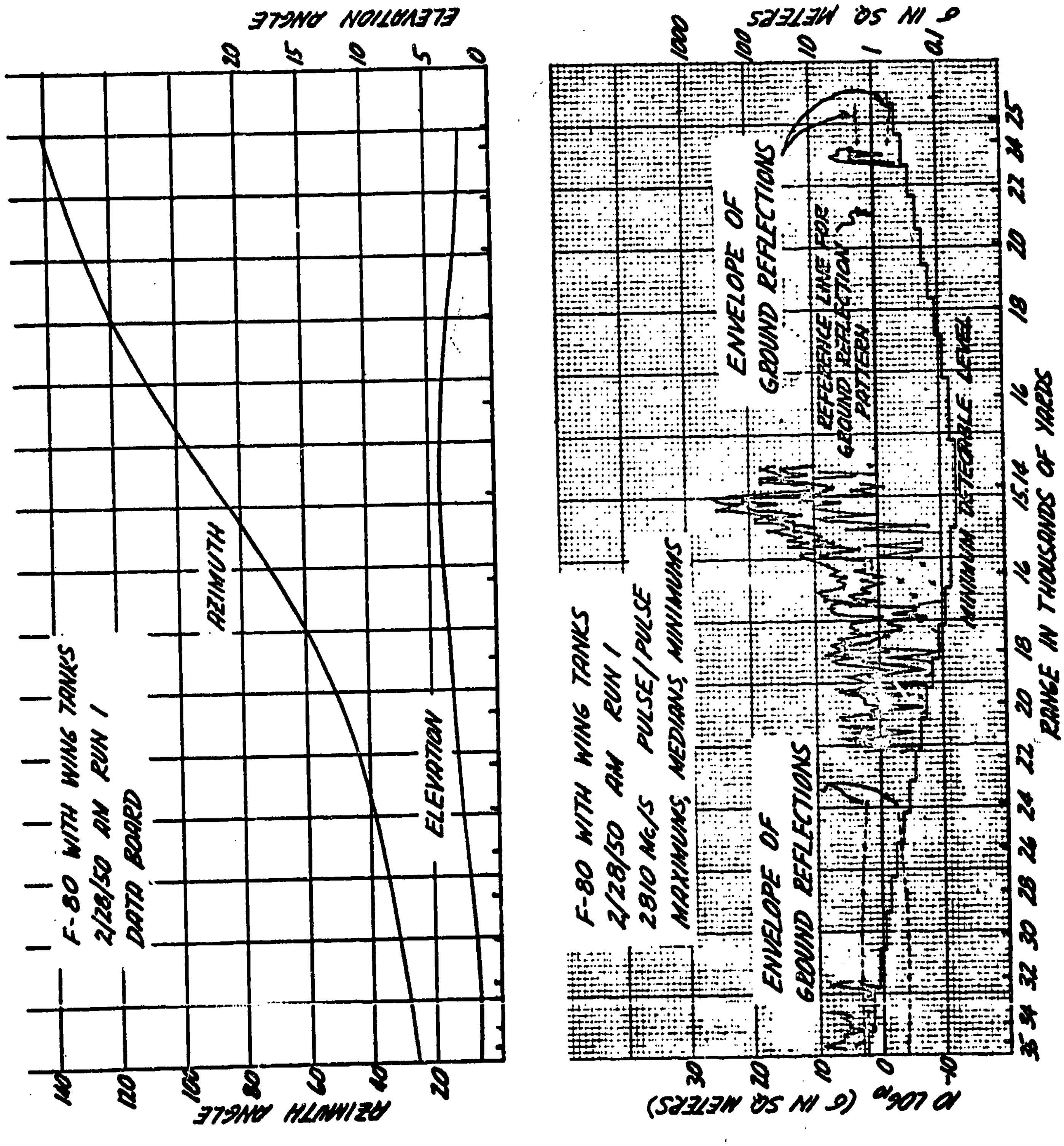
F-80 WITH WING TANKS
2/28/50 AM RUN I
DATA BOARD
AZIMUTH
ELEVATION
AZIMUTH ANGLE
ELEVATION ANGLE
140 120 100 80 60 40 20
0 5 10 15 20
F-80 WITH WING TANKS
2/28/50 AM RUN I
2810 Mc/S PULSE/PULSE
MAXIMUMS, MEDIANS, MINIMUMS
ENVELOPE OF GROUND REFLECTIONS
ENVELOPE OF GROUND REFLECTIONS
REFERENCE LINE FOR GROUND REFLECTION PATTERN
MINIMUM DETECTABLE LEVEL
RANGE IN THOUSANDS OF YARDS
σ IN SQ. METERS
1000 100 10 1 0.1
10 LOG10 (σ IN SQ. METERS)
30 20 10 0 -10

Figure 7

CONFIDENTIAL

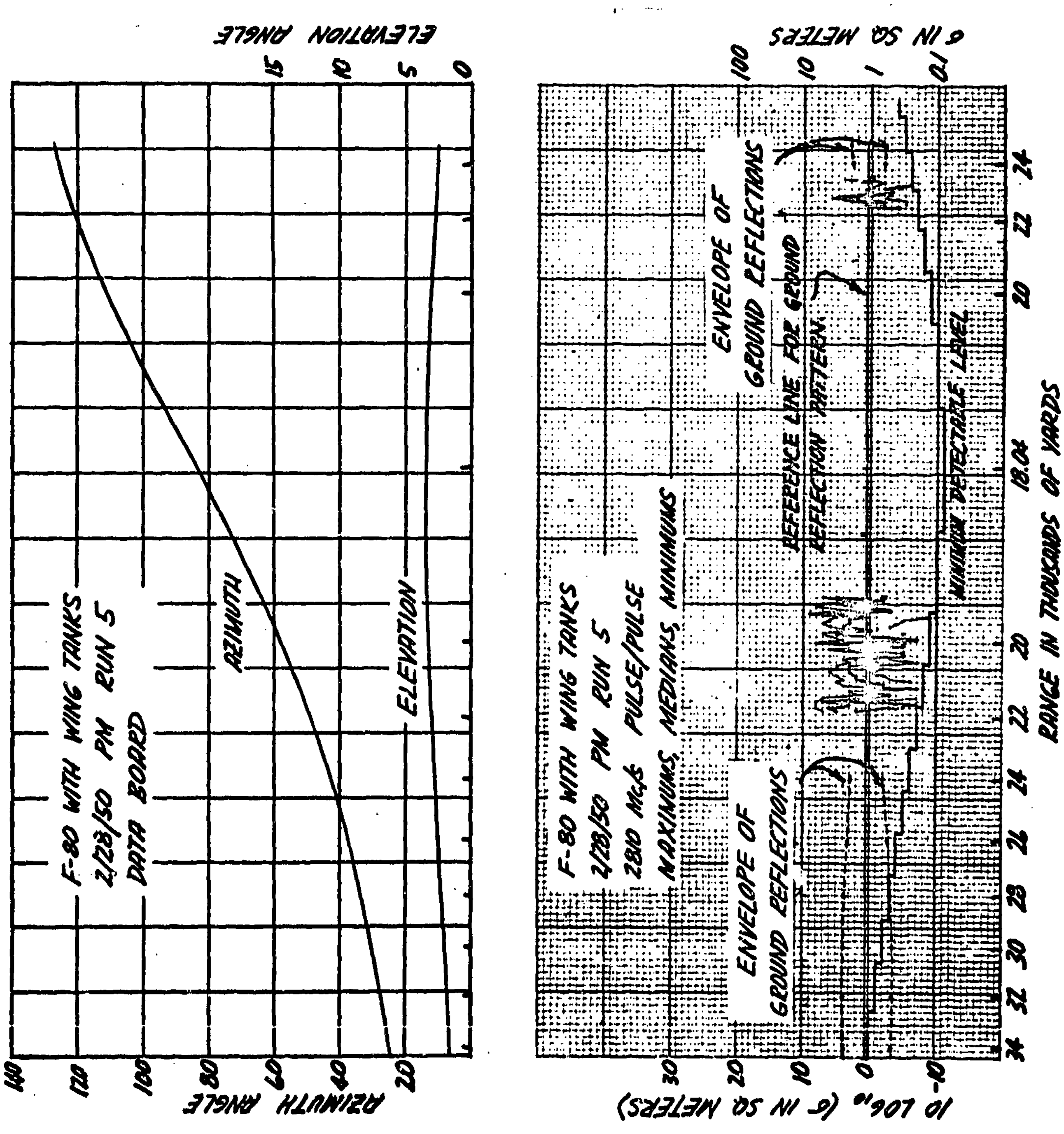

CONFIDENTIAL

Figure 8

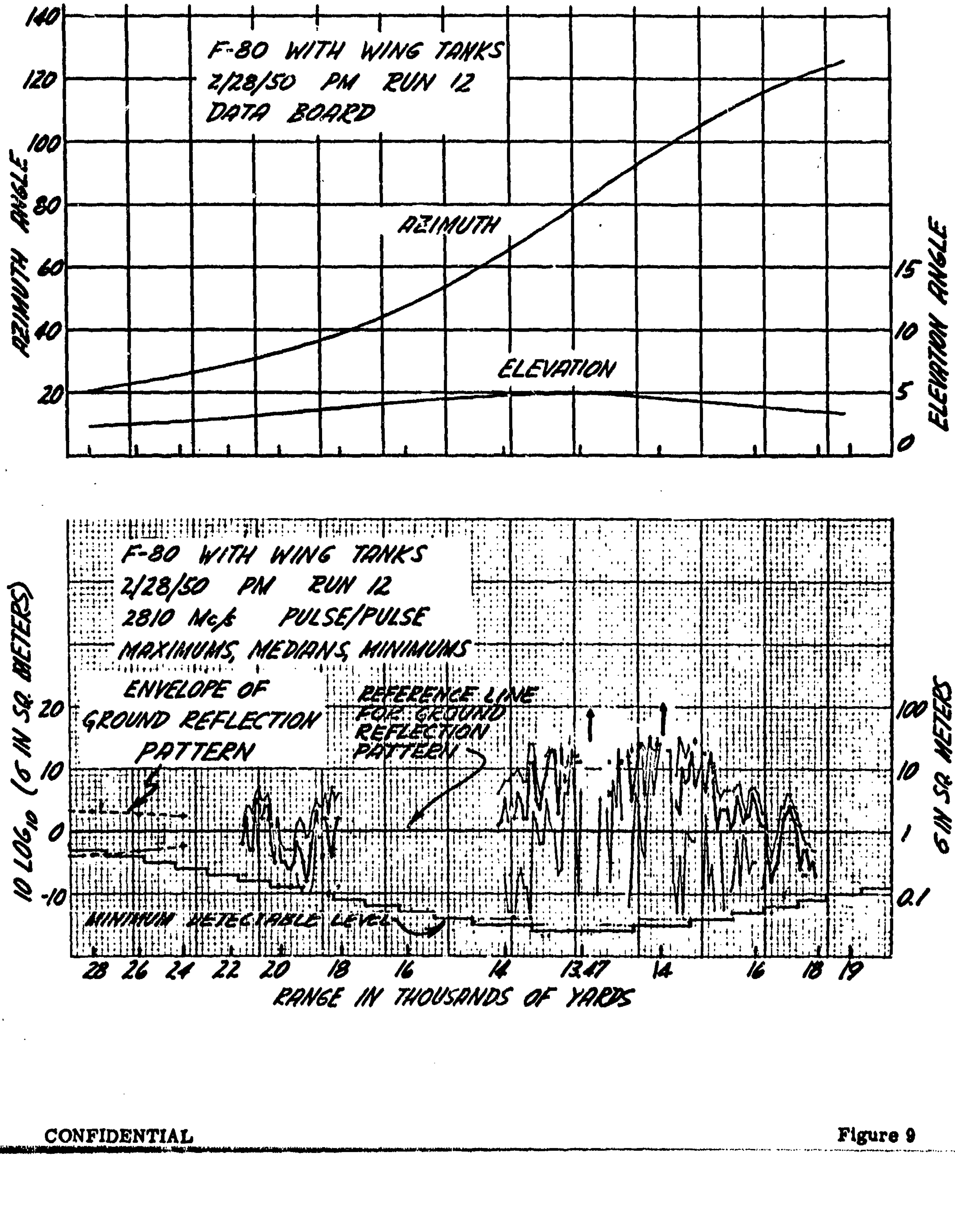
F-80 WITH WING TANKS
2/28/50 PM RUN 12
DATA BOARD
AZIMUTH ANGLE
ELEVATION ANGLE
AZIMUTH
ELEVATION
140
120
100
80
60
40
20
15
10
5
0
F-80 WITH WING TANKS
2/28/50 PM RUN 12
2810 Mc/s PULSE/PULSE
MAXIMUMS, MEDIANS, MINIMUMS
ENVELOPE OF GROUND REFLECTION PATTERN
REFERENCE LINE FOR GROUND REFLECTION PATTERN
MINIMUM DETECTABLE LEVEL
10 LOG10 (σ IN SQ. METERS)
σ IN SQ. METERS
20
10
0
-10
100
10
1
0.1
28 26 24 22 20 18 16 14 13.47 14 16 18 19
RANGE IN THOUSANDS OF YARDS

Figure 9

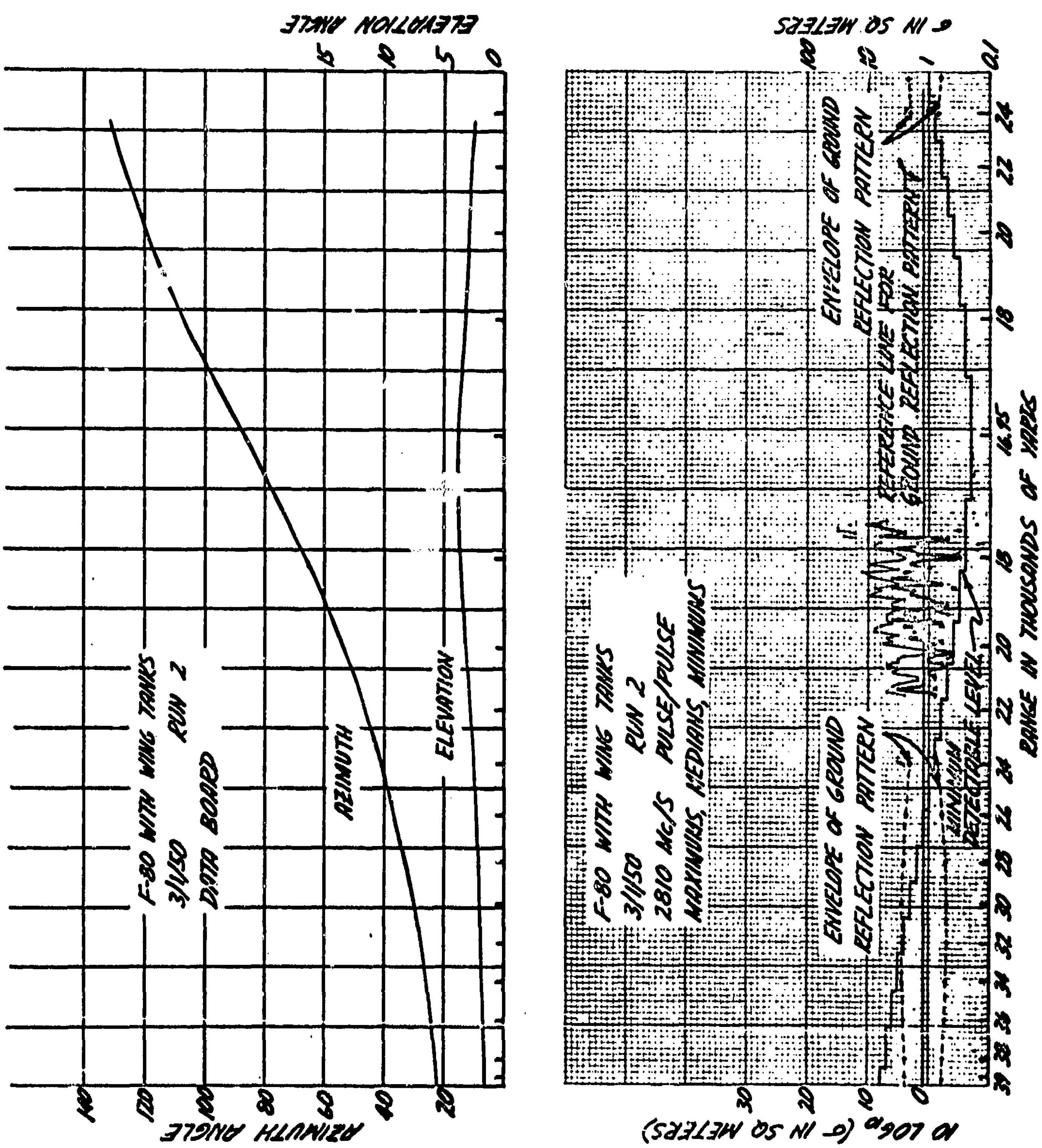
ELEVATION ANGLE
AZIMUTH ANGLE
F-80 WITH WING TANKS
3/1/50 RUN 2
DATA BOARD
AZIMUTH
ELEVATION
σ IN SQ METERS
10 LOG10 (σ IN SQ METERS)
F-80 WITH WING TANKS
3/1/50 RUN 2
2810 Mc/S PULSE/PULSE
MAXIMUMS, MEDIANS, MINIMUMS
ENVELOPE OF GROUND REFLECTION PATTERN
REFERENCE LINE FOR GROUND REFLECTION PATTERN
ENVELOPE OF GROUND REFLECTION PATTERN
MINIMUM DETECTABLE LEVEL
RANGE IN THOUSANDS OF YARDS

Figure 10

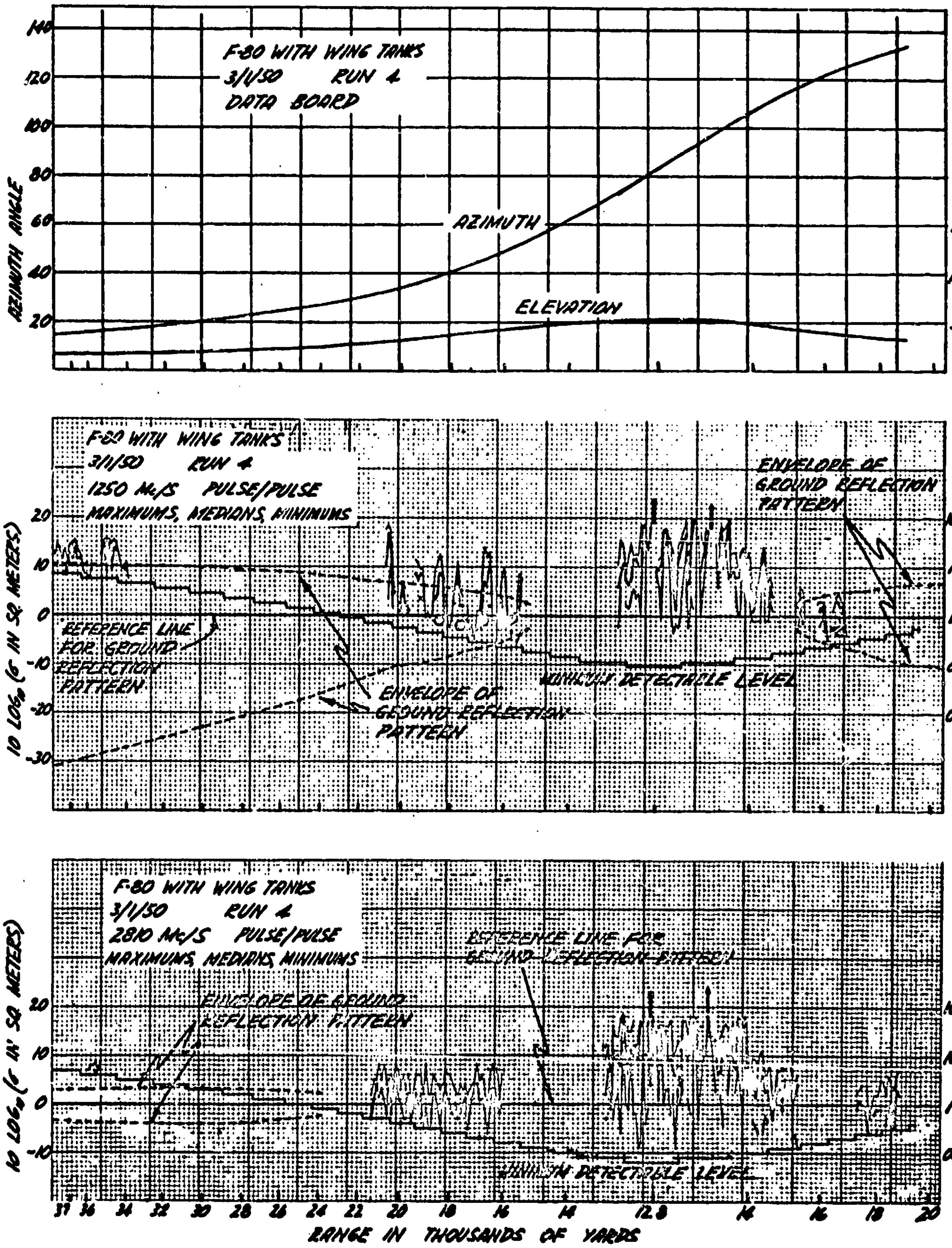
F-80 WITH WING TANKS
3/1/50 RUN 4
DATA BOARD
AZIMUTH ANGLE
ELEVATION ANGLE
AZIMUTH
ELEVATION
F-80 WITH WING TANKS
3/1/50 RUN 4
1250 Mc/S PULSE/PULSE
MAXIMUMS, MEDIANS, MINIMUMS
REFERENCE LINE FOR GROUND REFLECTION PATTERN
ENVELOPE OF GROUND REFLECTION PATTERN
MINIMUM DETECTABLE LEVEL
10 LOG10 (σ IN SQ METERS)
σ IN SQ METERS
F-80 WITH WING TANKS
3/1/50 RUN 4
2810 Mc/S PULSE/PULSE
MAXIMUMS, MEDIANS, MINIMUMS
REFERENCE LINE FOR GROUND REFLECTION PATTERN
ENVELOPE OF GROUND REFLECTION PATTERN
MINIMUM DETECTABLE LEVEL
RANGE IN THOUSANDS OF YARDS

Figure 11

CONFIDENTIAL

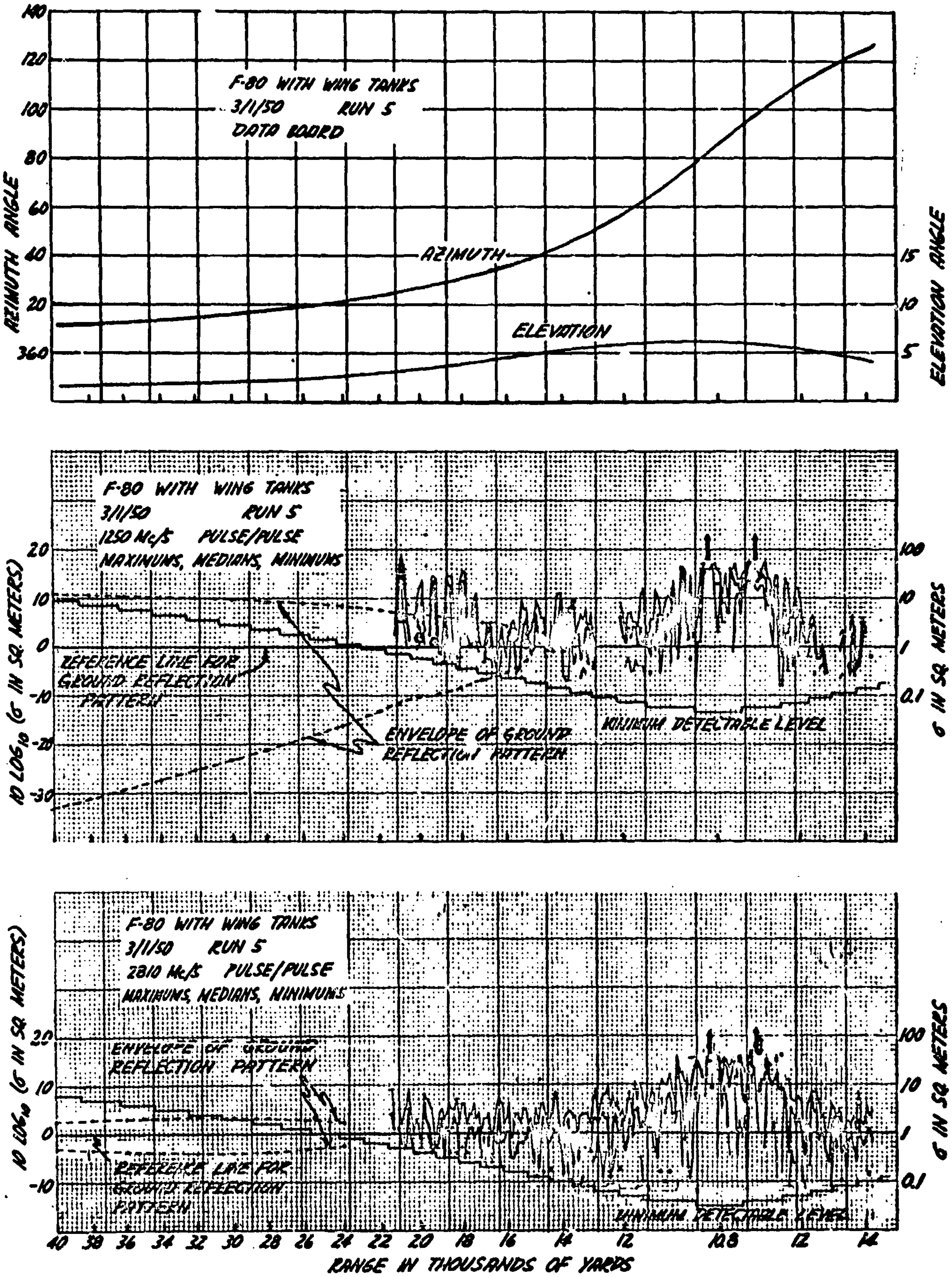

Figure 12

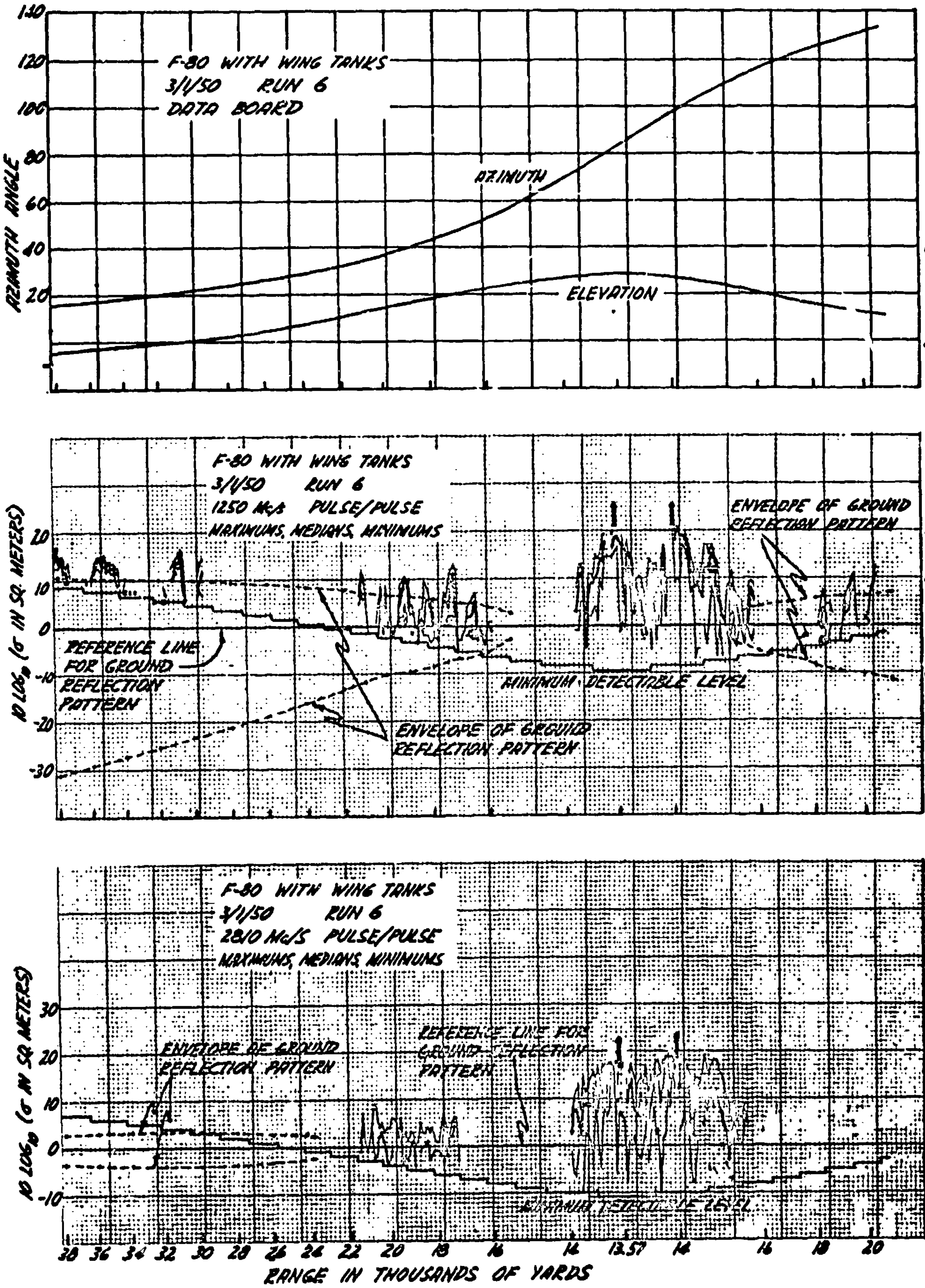
F-80 WITH WING TANKS
3/1/50 RUN 6
DATA BOARD
AZIMUTH
ELEVATION
AZIMUTH ANGLE
ELEVATION ANGLE
F-80 WITH WING TANKS
3/1/50 RUN 6
1250 Mc/s PULSE/PULSE
MAXIMUMS, MEDIANS, MINIMUMS
ENVELOPE OF GROUND REFLECTION PATTERN
REFERENCE LINE FOR GROUND REFLECTION PATTERN
MINIMUM DETECTABLE LEVEL
ENVELOPE OF GROUND REFLECTION PATTERN
10 LOG10 (σ IN SQ. METERS)
σ IN SQ METERS
F-80 WITH WING TANKS
3/1/50 RUN 6
2810 Mc/S PULSE/PULSE
MAXIMUMS, MEDIANS, MINIMUMS
ENVELOPE OF GROUND REFLECTION PATTERN
REFERENCE LINE FOR GROUND REFLECTION PATTERN
10 LOG10 (σ IN SQ METERS)
σ IN SQ METERS
RANGE IN THOUSANDS OF YARDS

Figure 13

CONFIDENTIAL

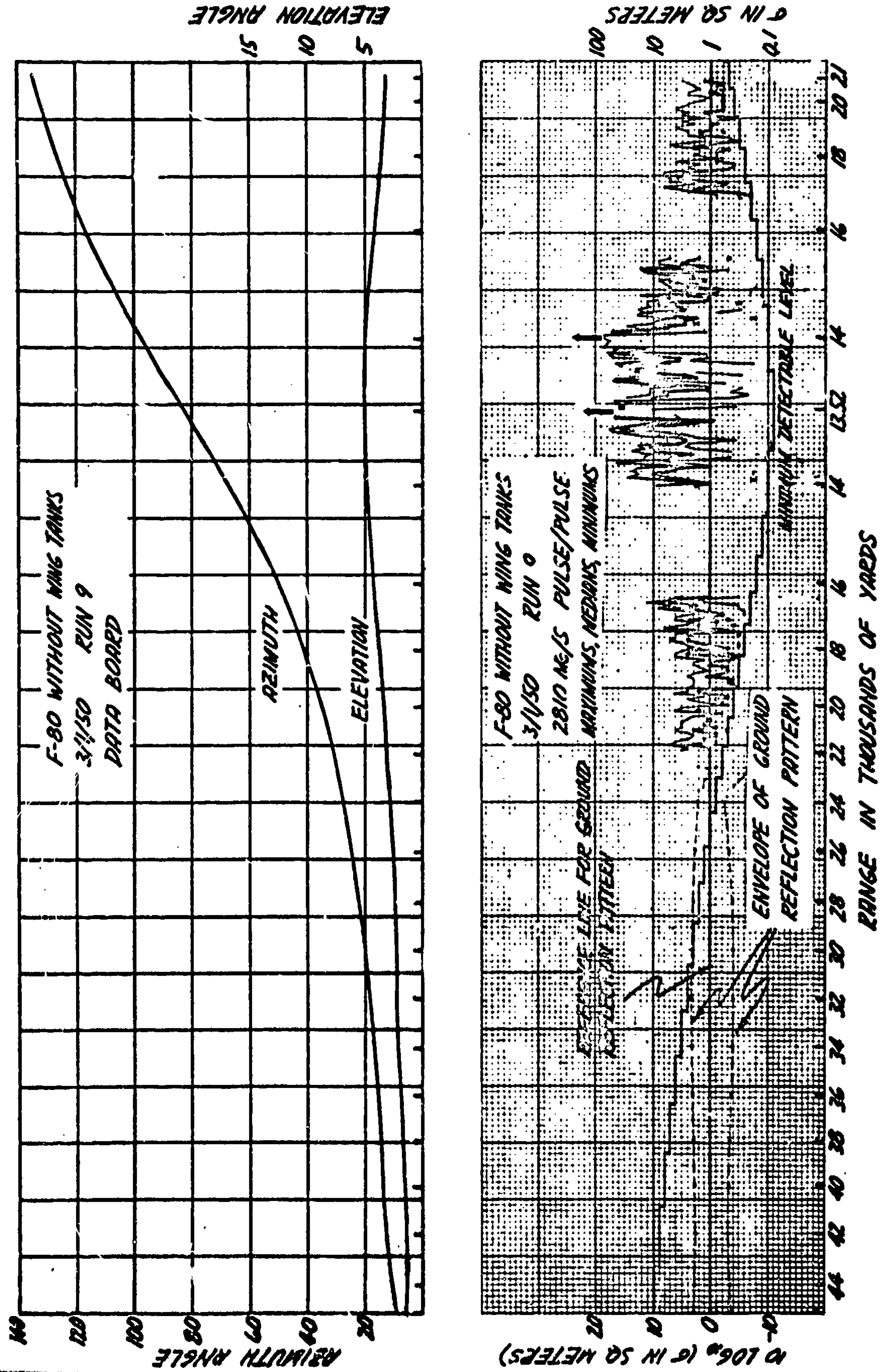

CONFIDENTIAL

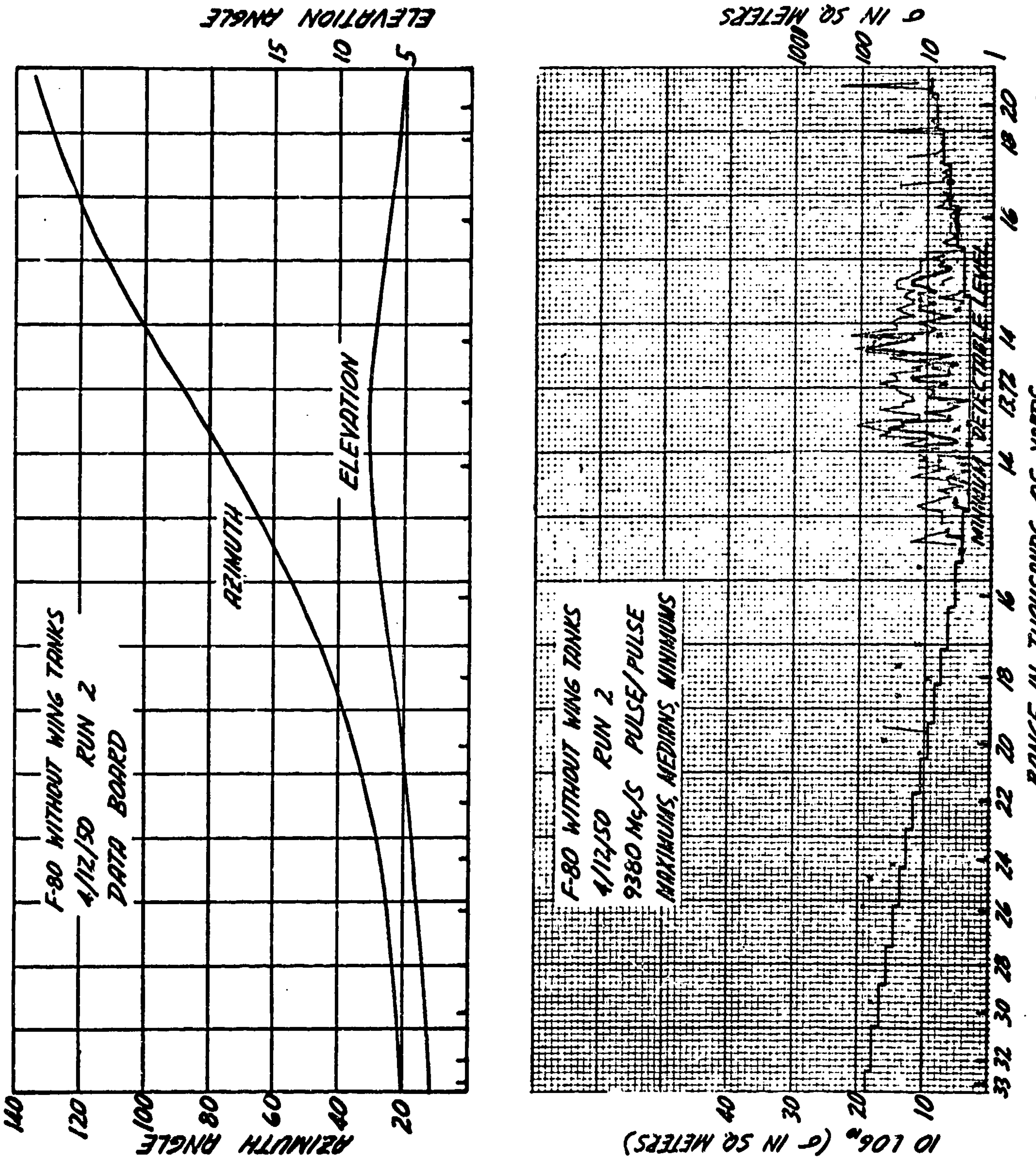

Figure 15

CONFIDENTIAL

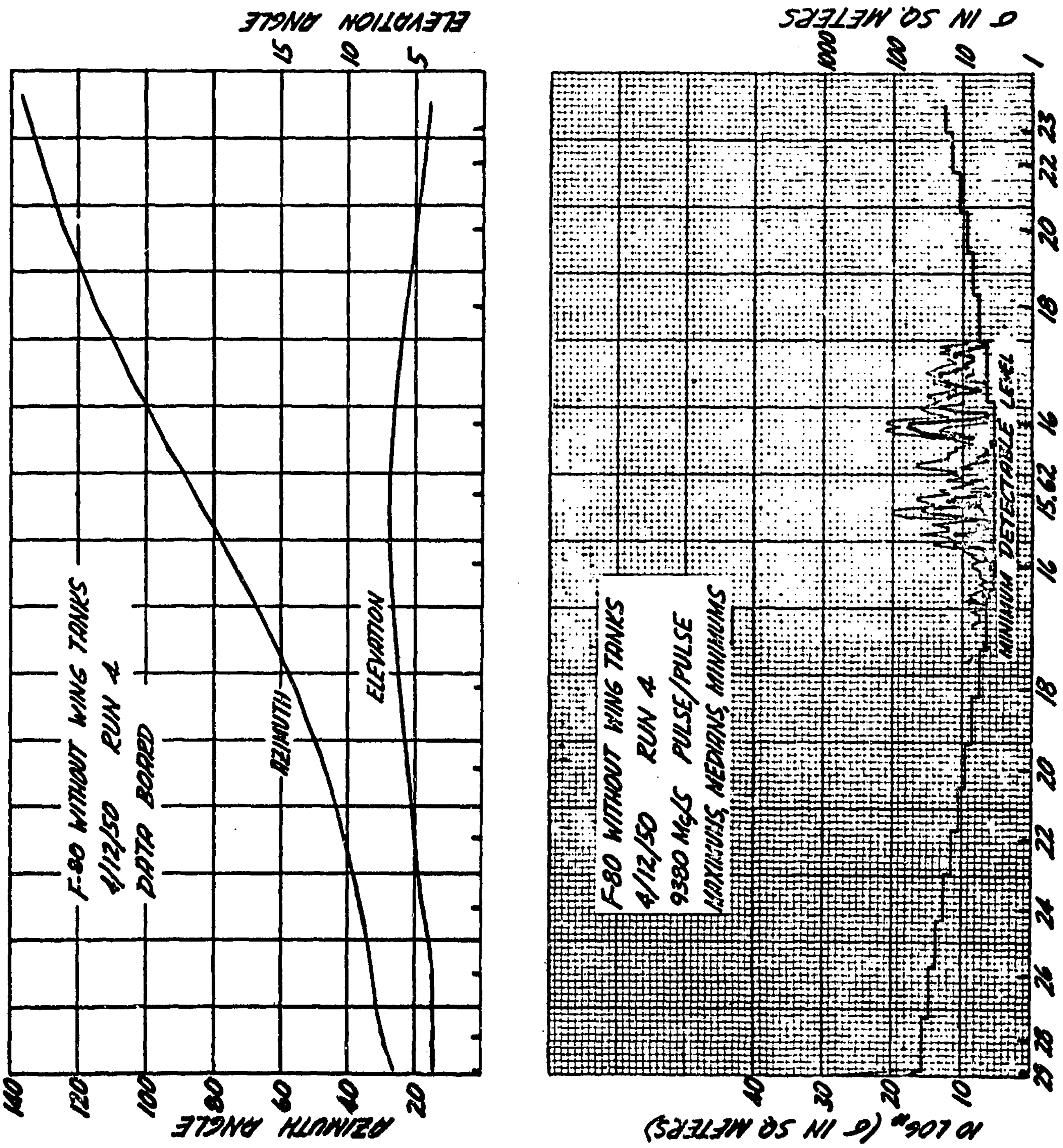

Figure 16

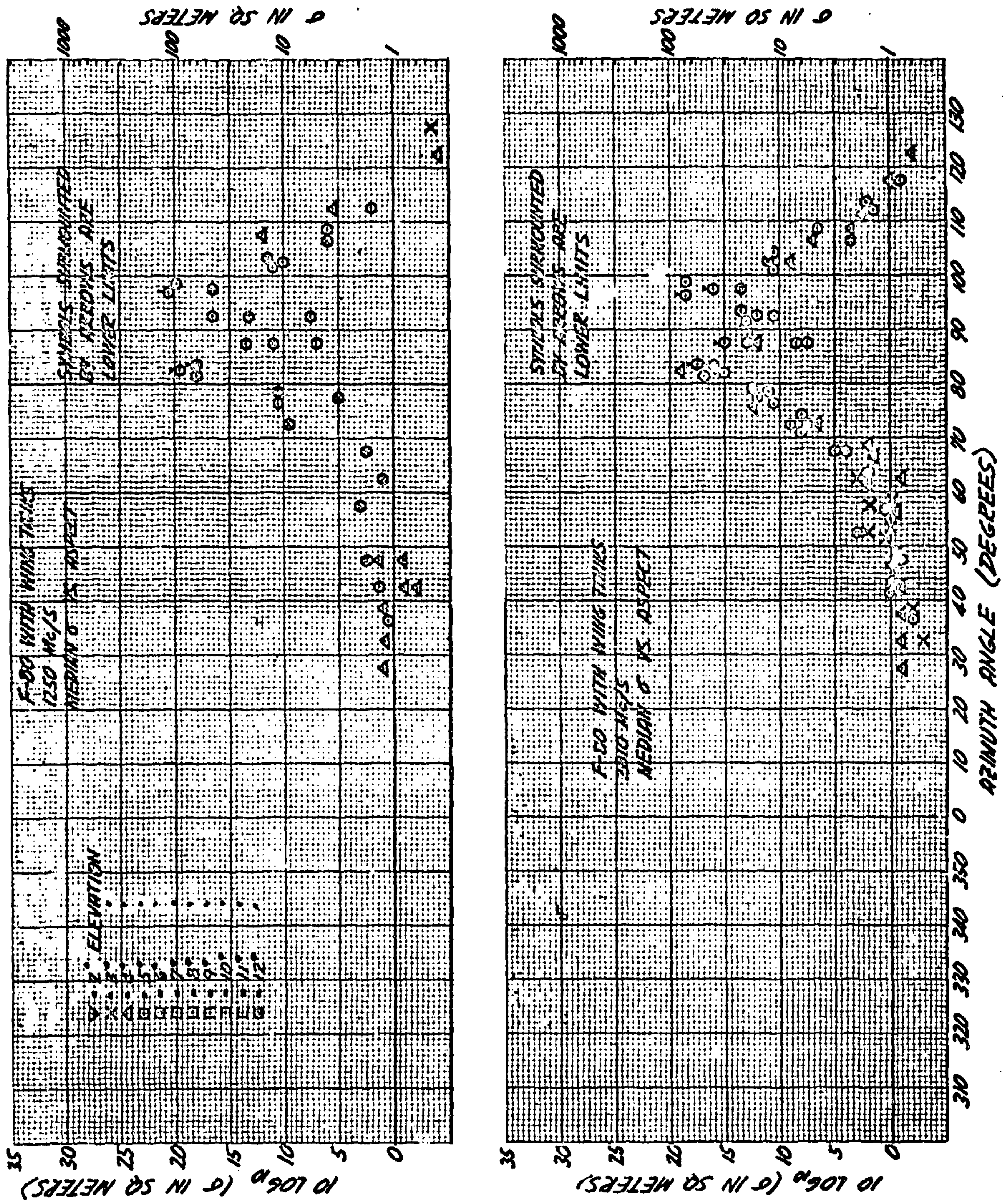
F-80 WITH WING TANKS
1250 Mc/S
MEDIAN σ VS ASPECT
SYMBOLS SURMOUNTED BY ARROWS ARE LOWER LIMITS
ELEVATION
σ IN SQ METERS
10 LOG10 (σ IN SQ METERS)
F-80 WITH WING TANKS
MEDIAN σ VS ASPECT
SYMBOLS SURMOUNTED BY ARROWS ARE LOWER LIMITS
σ IN SQ METERS
10 LOG10 (σ IN SQ METERS)
AZIMUTH ANGLE (DEGREES)

Figure 17

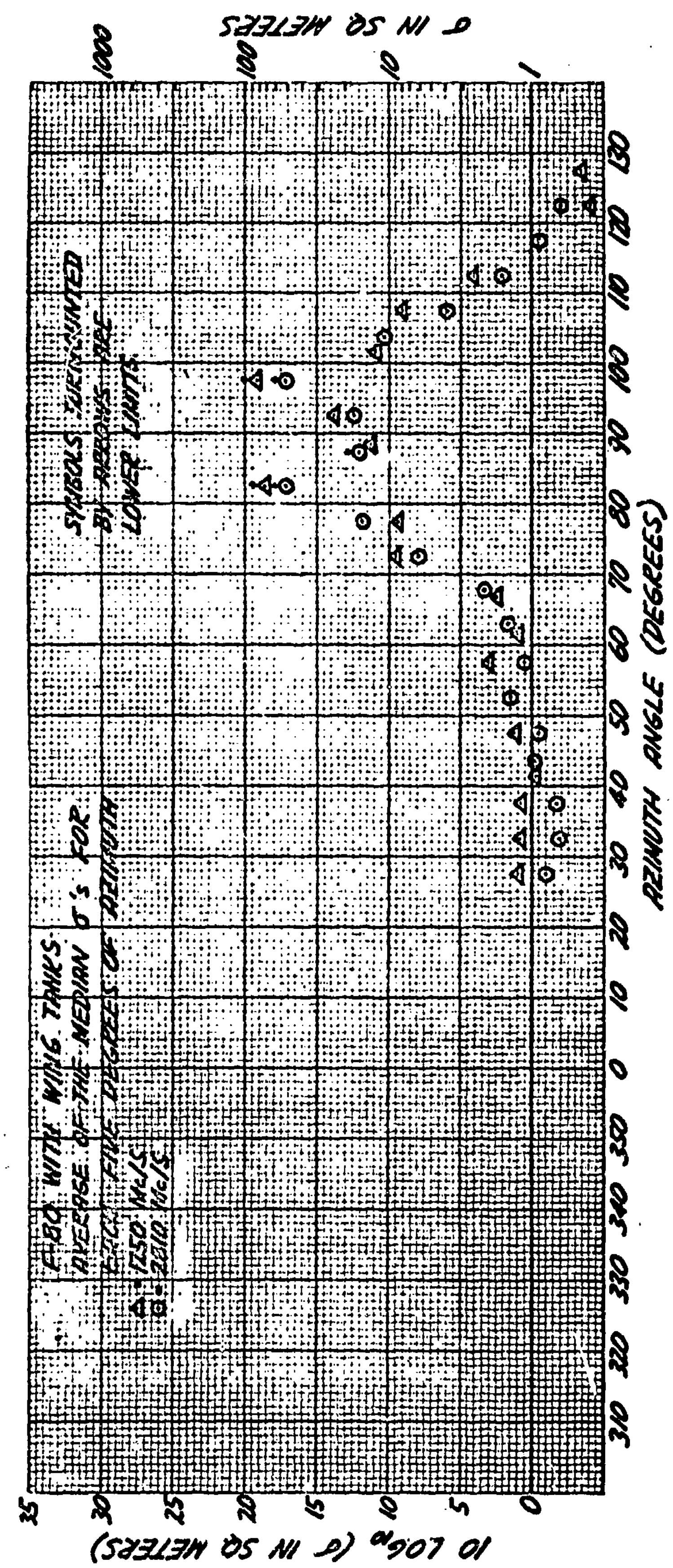
F-80 WITH WING TANKS
AVERAGE OF THE MEDIAN σ's FOR
FIVE DEGREES OF AZIMUTH
Δ: 1250 Mc/S
⊙: 2810 Mc/S
SYMBOLS SURMOUNTED
BY ARROWS ARE
LOWER LIMITS
σ IN SQ METERS
10 LOG10 (σ IN SQ METERS)
AZIMUTH ANGLE (DEGREES)

Figure 18

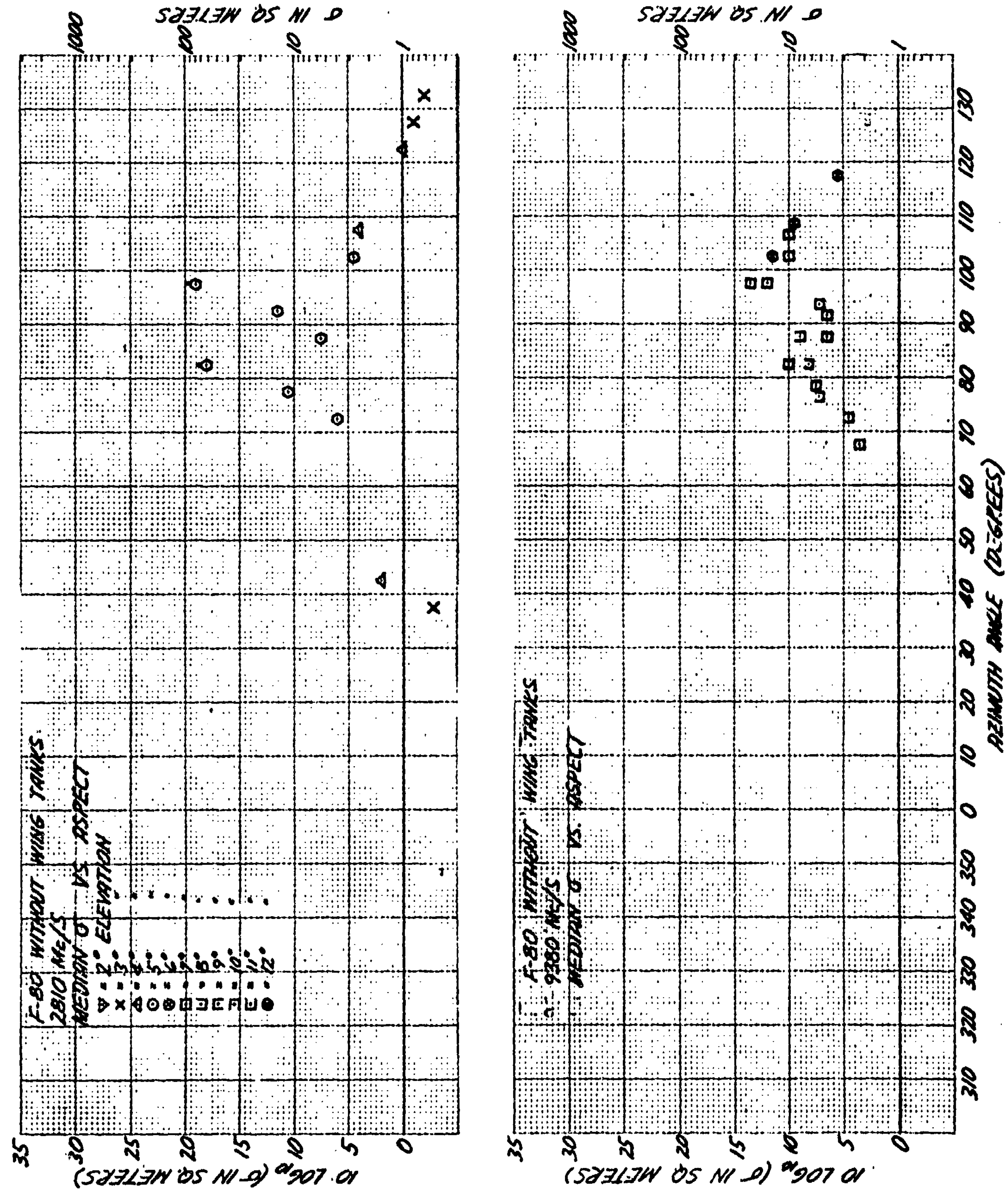

F-80 WITHOUT WING TANKS
2810 Mc/S
MEDIAN σ VS. ASPECT
ELEVATION
F-80 WITHOUT WING TANKS
9380 Mc/S
MEDIAN σ VS. ASPECT
σ IN SQ METERS
10 LOG10 (σ IN SQ METERS)
AZIMUTH ANGLE (DEGREES)

Figure 19

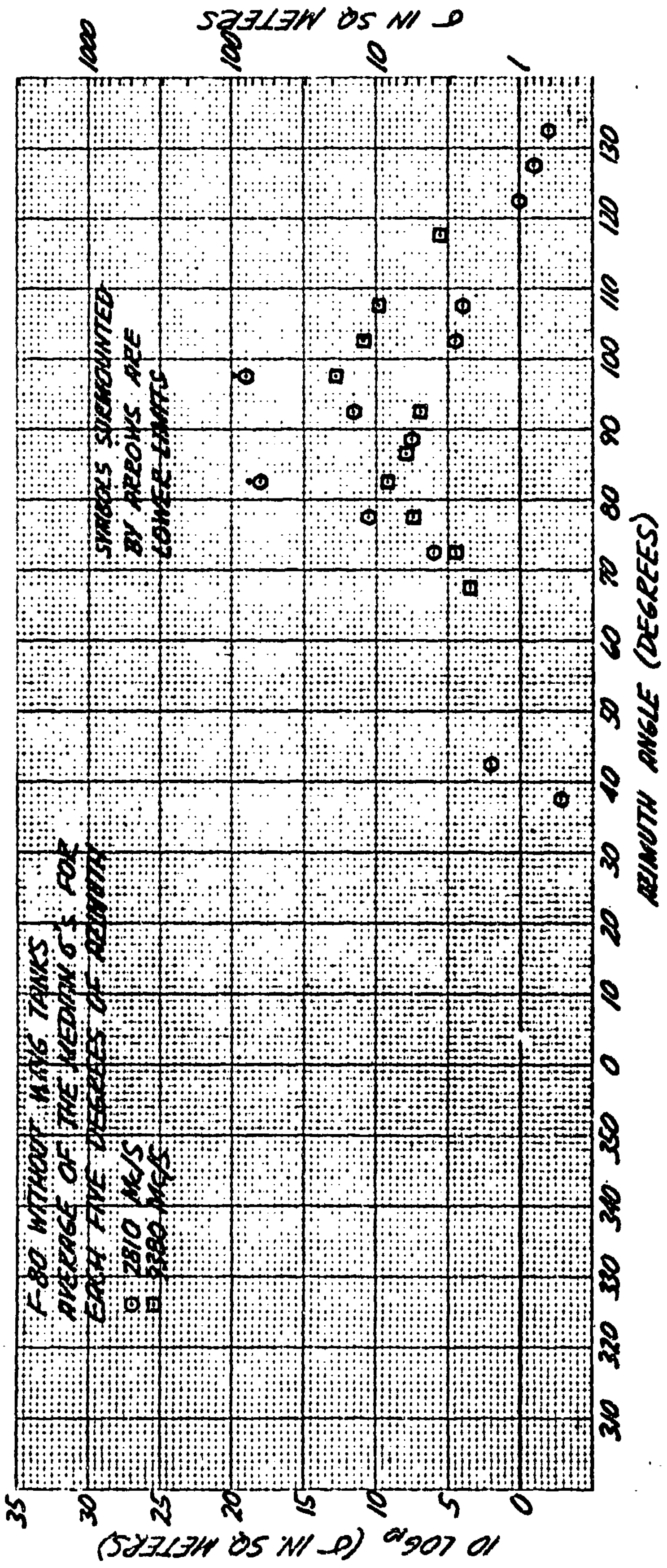

F-80 WITHOUT WING TANKS
AVERAGE OF THE MEDIAN σ'S FOR
EACH FIVE DEGREES OF AZIMUTH
2810 MC/S
9380 MC/S
SYMBOLS SURMOUNTED
BY ARROWS ARE
LOWER LIMITS
σ IN SQ METERS
1000
100
10
1
AZIMUTH ANGLE (DEGREES)
10 LOG10 (σ IN SQ METERS)

Figure 20

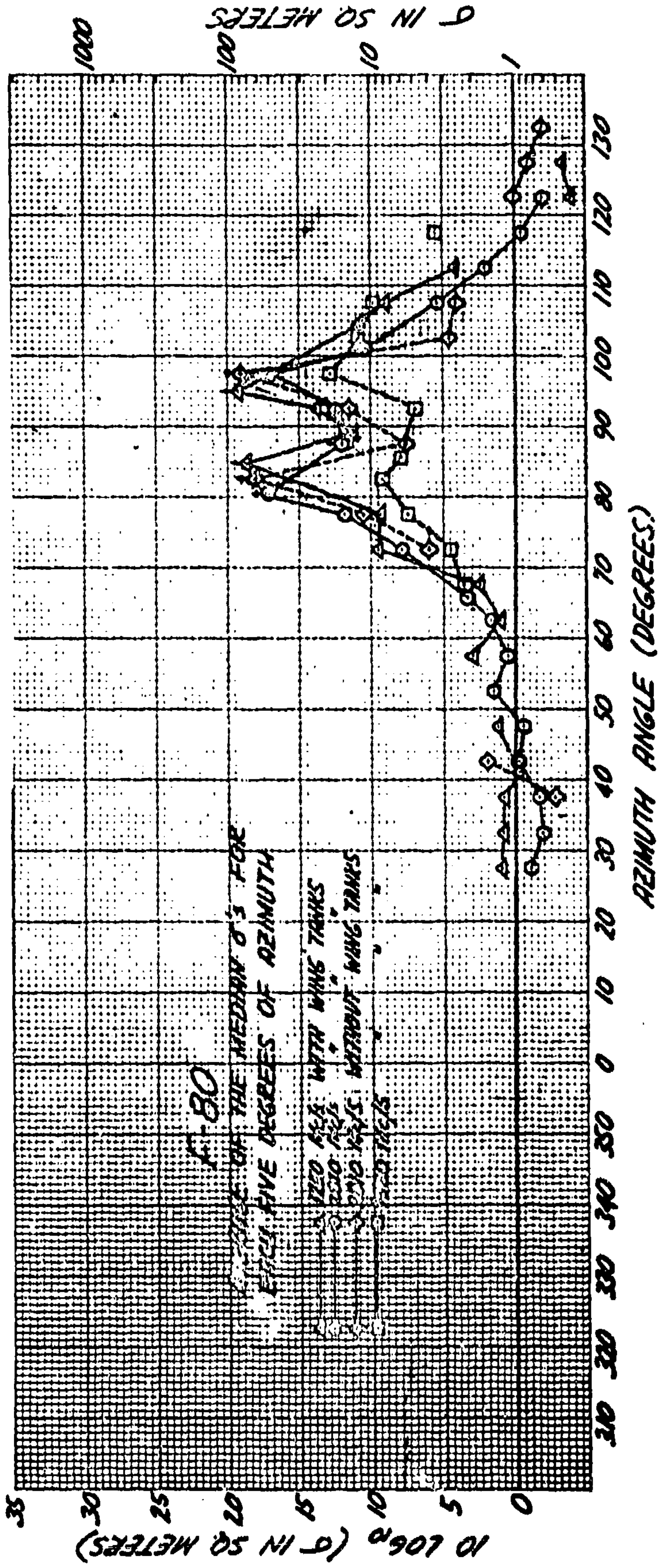
F-80
OF THE MEDIAN σ's FOR
EACH FIVE DEGREES OF AZIMUTH
WITH WING TANKS
WITHOUT WING TANKS
σ IN SQ METERS
10 LOG10 (σ IN SQ METERS)
AZIMUTH ANGLE (DEGREES)

Figure 21

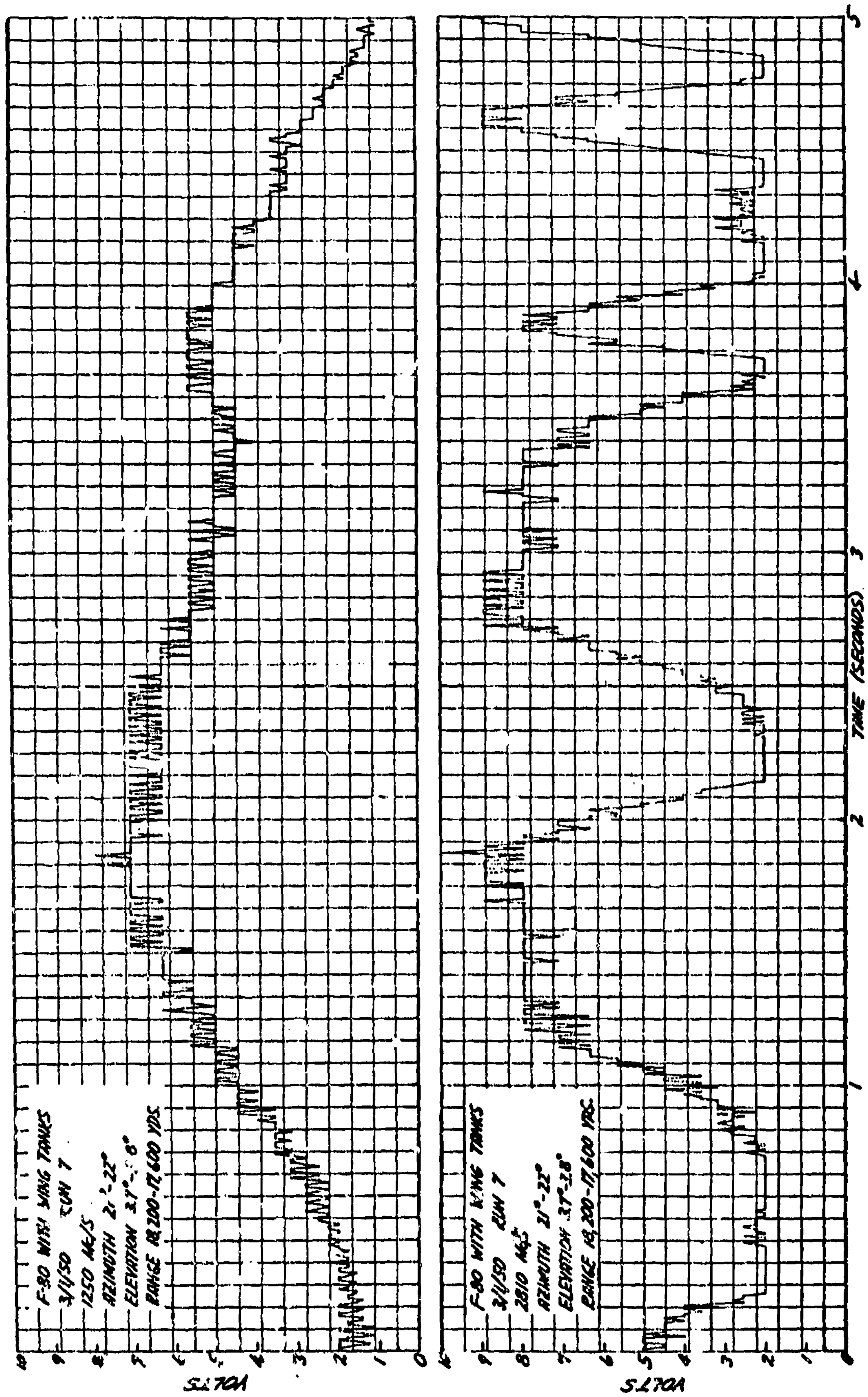
F-80 WITH WING TANKS
3/1/50 RUN 7
1250 MC/S
AZIMUTH 21°-22°
RANGE 18,200-17,600 YDS
VOLTS
F-80 WITH WING TANKS
3/1/50 RUN 7
2810 MC/S
AZIMUTH 21°-22°
ELEVATION 3.7°-3.8°
RANGE 18,200-17,600 YDS
VOLTS
TIME (SECONDS)

Figure 22

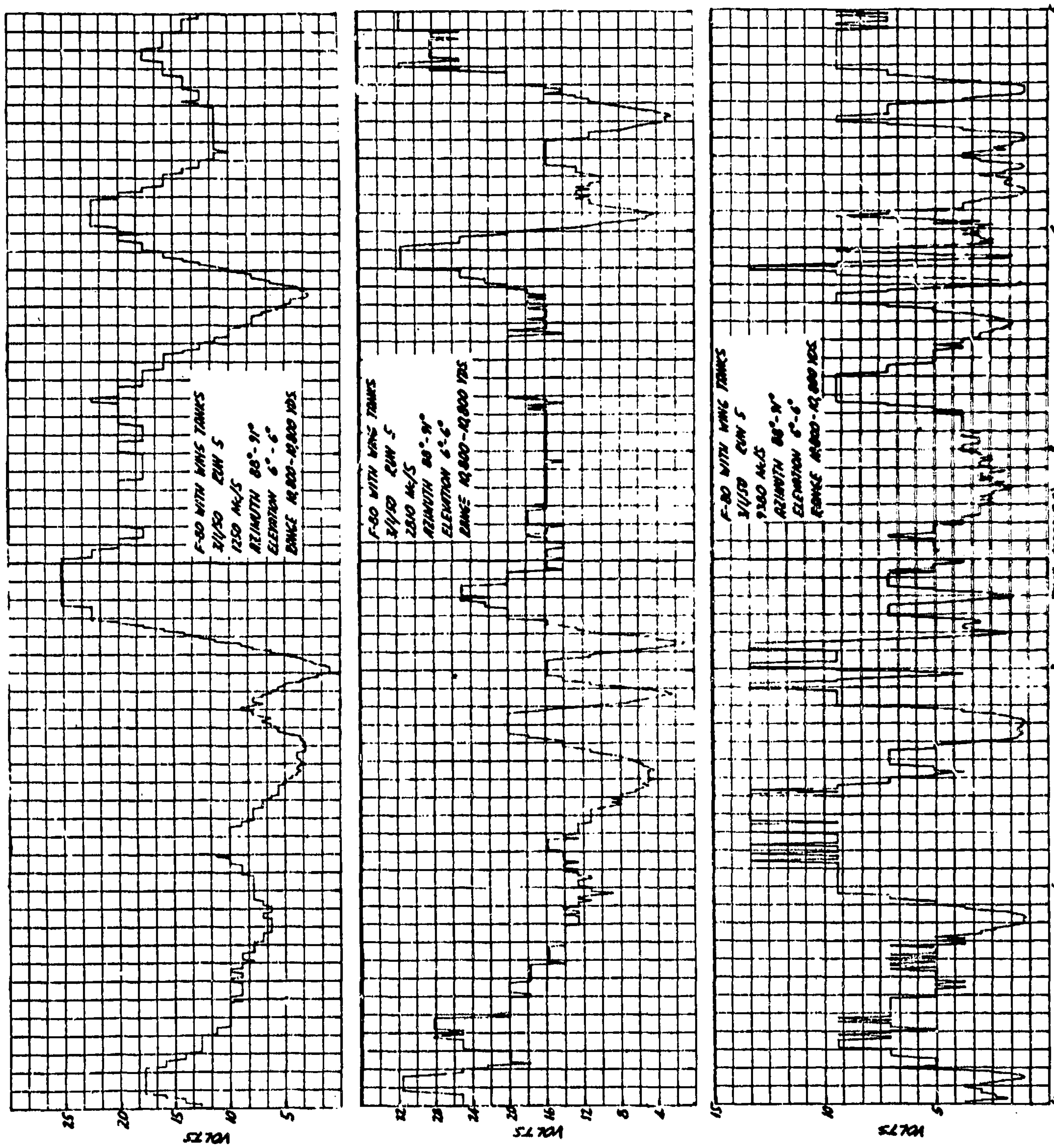

Figure 23

CONFIDENTIAL

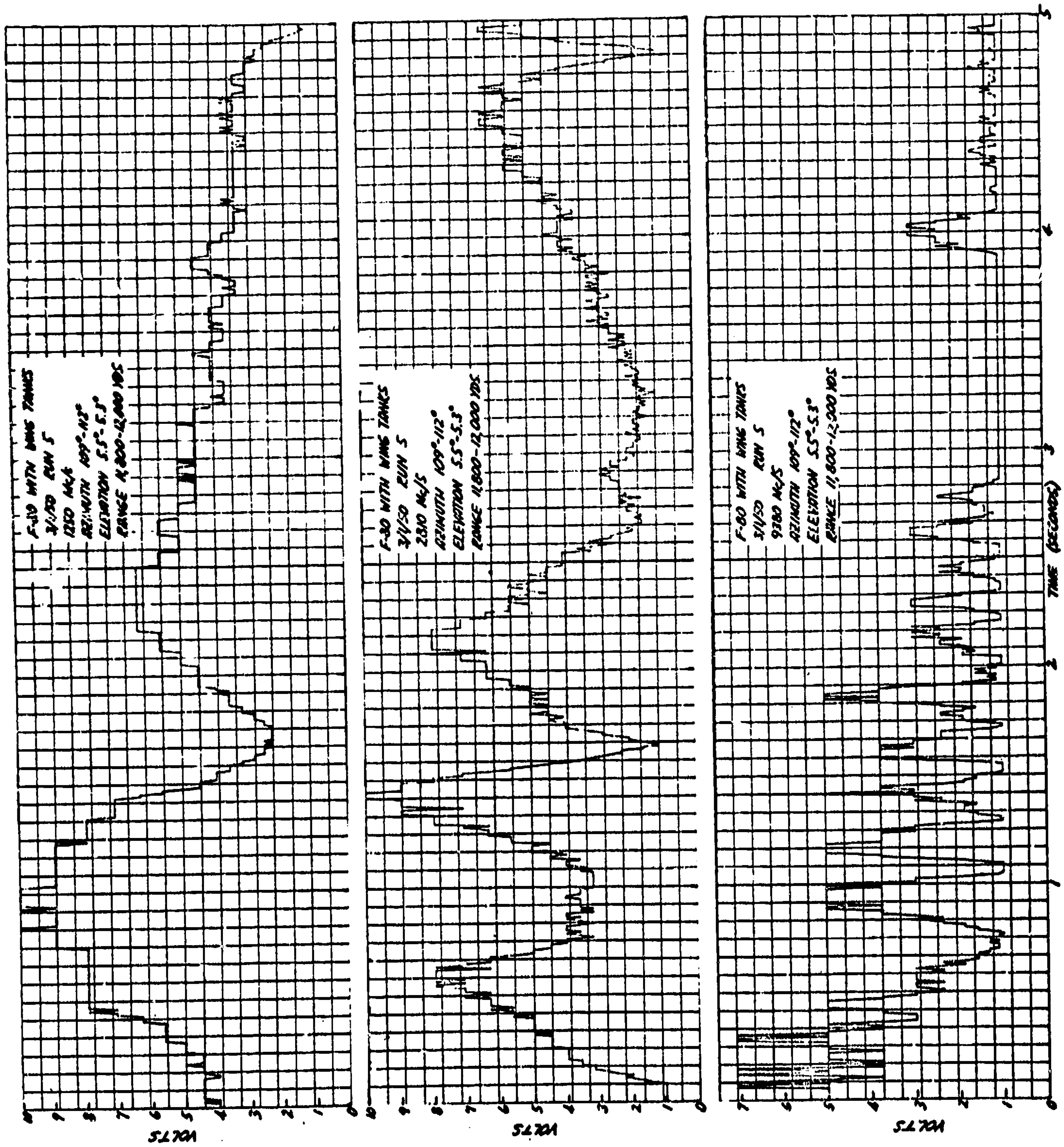

Figure 24

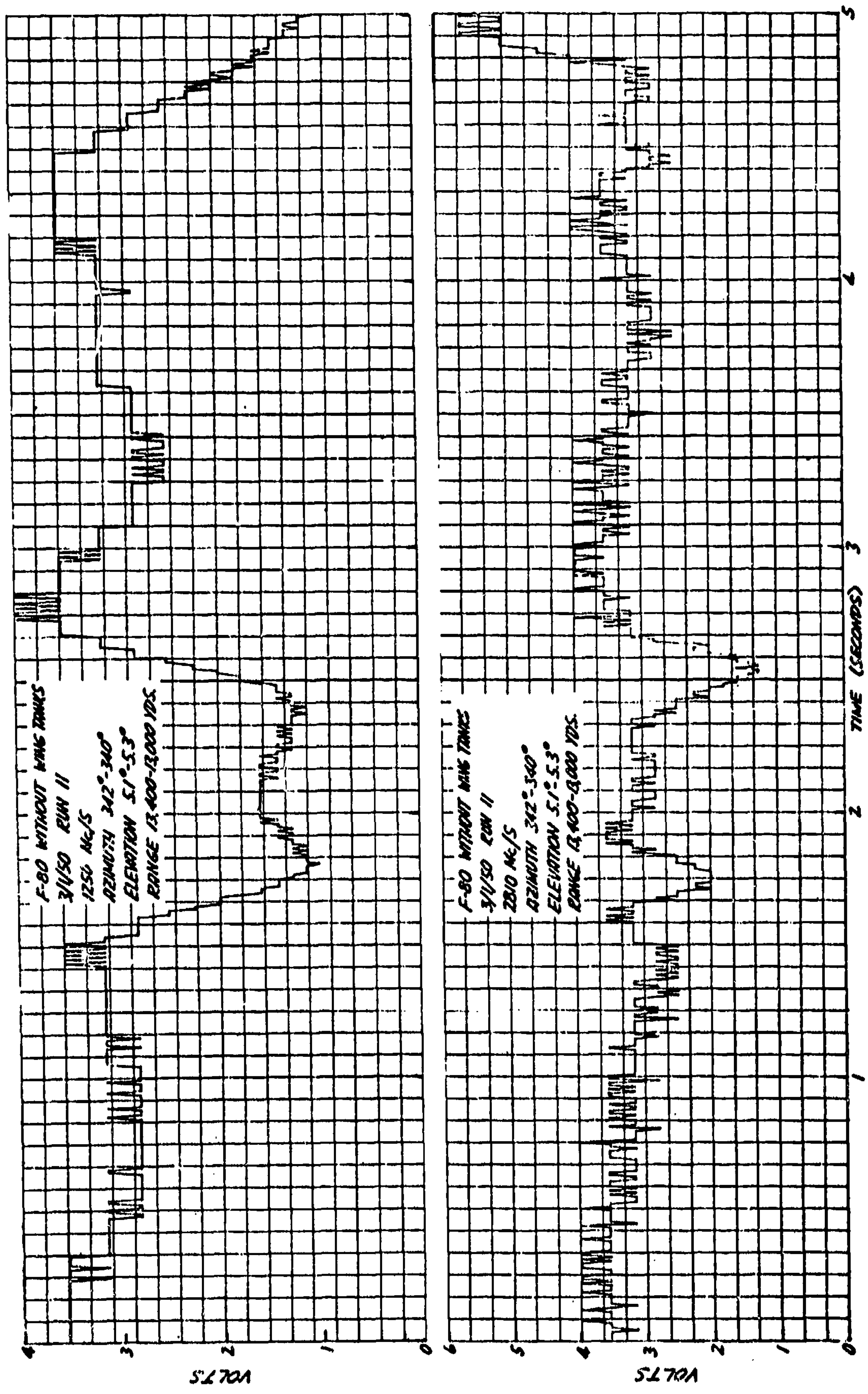
F-80 WITHOUT WING TANKS
3/1/50 RUN 11
1250 Mc/S
AZIMUTH 342°-340°
ELEVATION 5.1°-5.3°
RANGE 13,400-13,000 YDS.
VOLTS
F-80 WITHOUT WING TANKS
3/1/50 RUN 11
2810 Mc/S
AZIMUTH 342°-340°
ELEVATION 5.1°-5.3°
RANGE 13,400-13,000 YDS.
VOLTS
TIME (SECONDS)

Figure 25

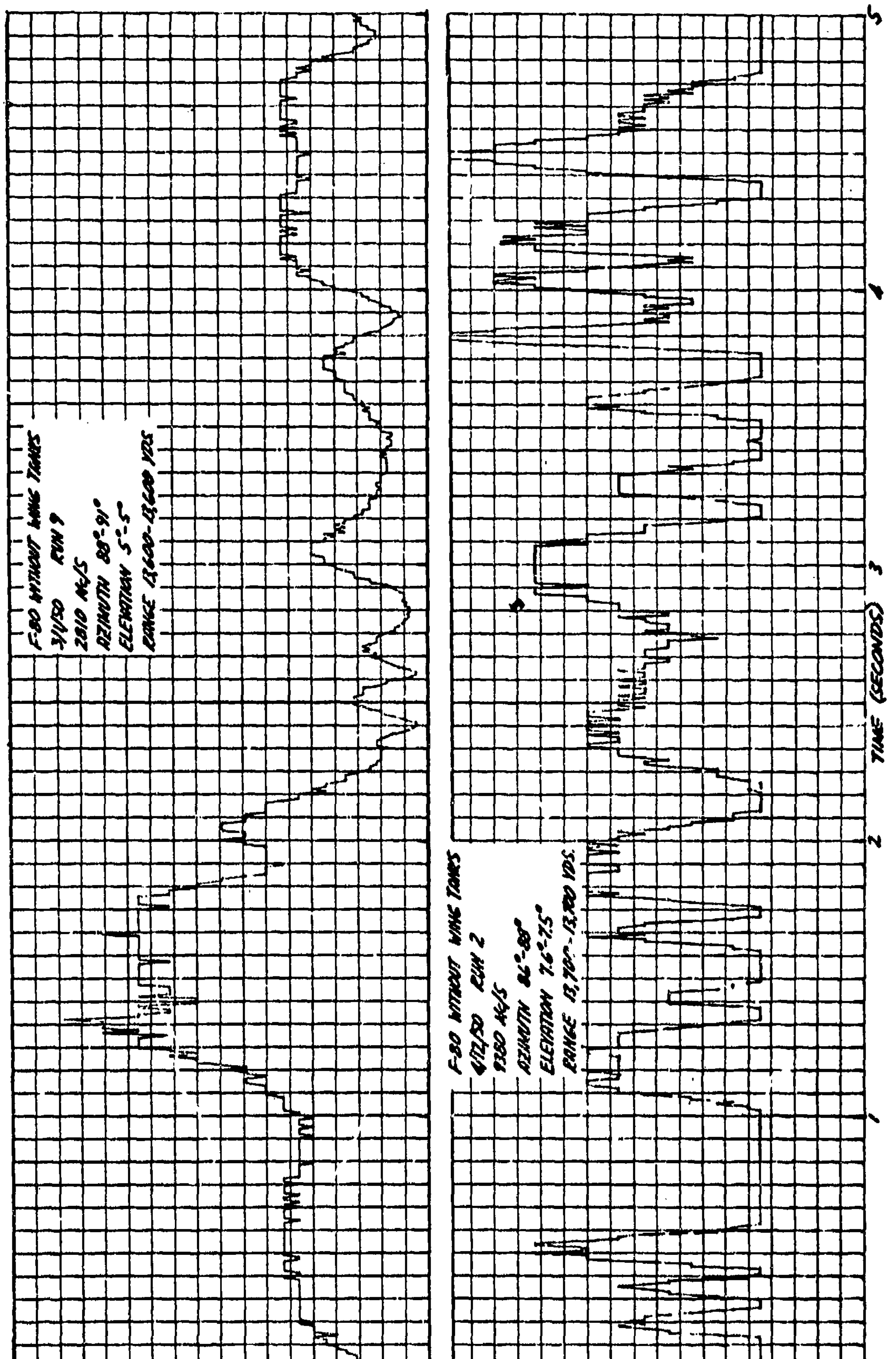
F-80 WITHOUT WING TANKS
3/1/50 RUN 9
2810 Mc/S
AZIMUTH 88°-91°
ELEVATION 5°-5°
RANGE 13,600-13,600 YDS
F-80 WITHOUT WING TANKS
4/12/50 RUN 2
9380 Mc/S
AZIMUTH 86°-88°
ELEVATION 7.6°-7.5°
RANGE 13,700-13,700 YDS.
TIME (SECONDS)
0 1 2 3 4 5
32 28 24 20 16 12 8 4 0
4 3 2 1 0

Figure 26

CONFIDENTIAL

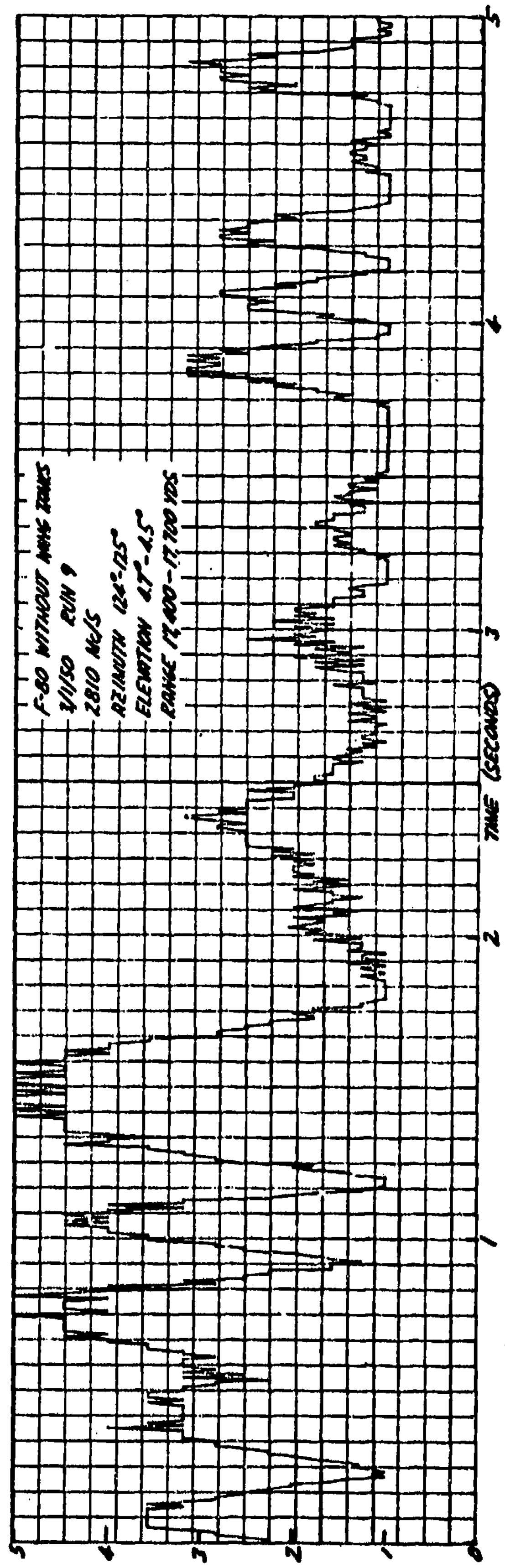

CONFIDENTIAL

Figure 27

CONFIDENTIAL

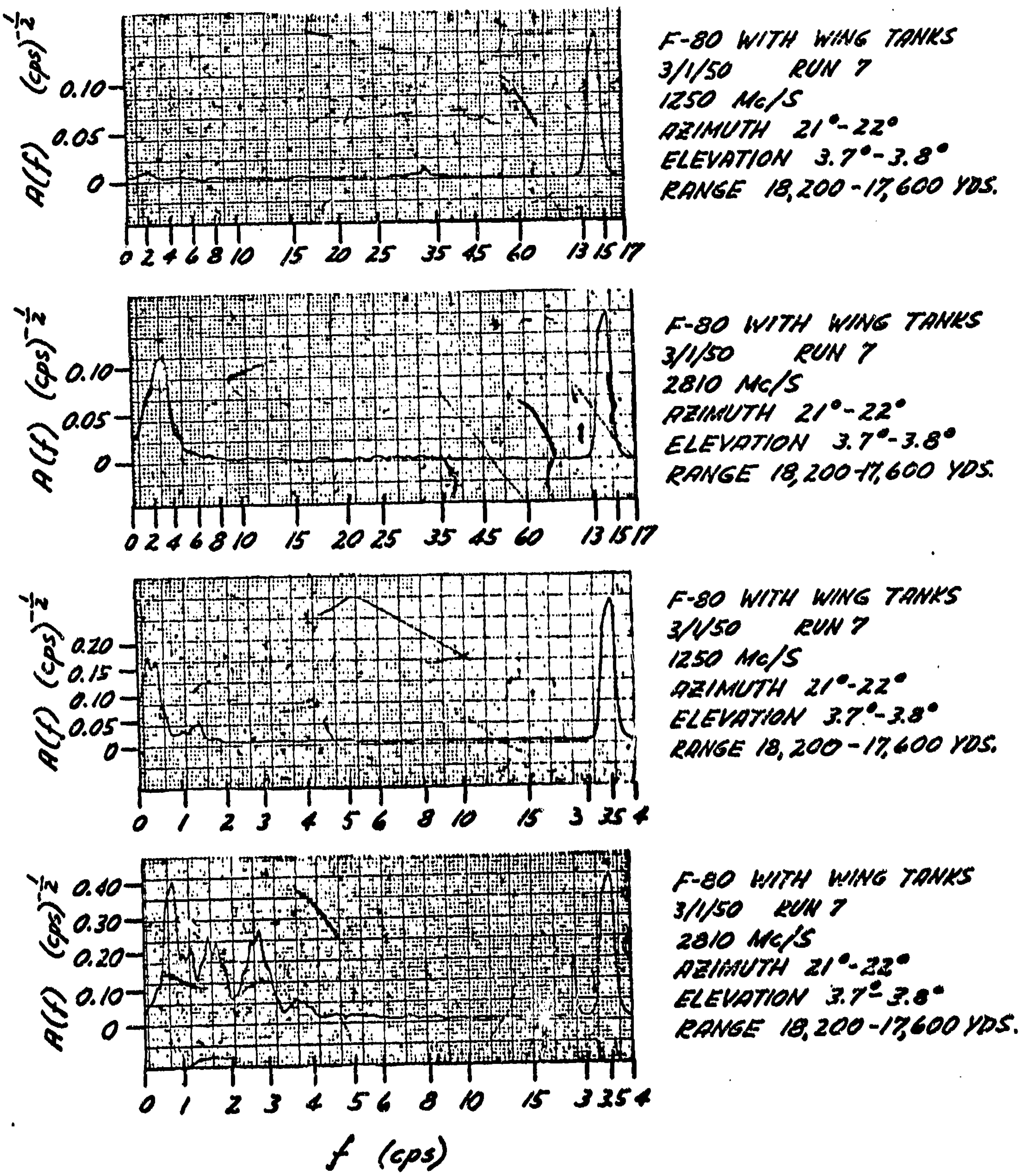

CONFIDENTIAL

Figure 28

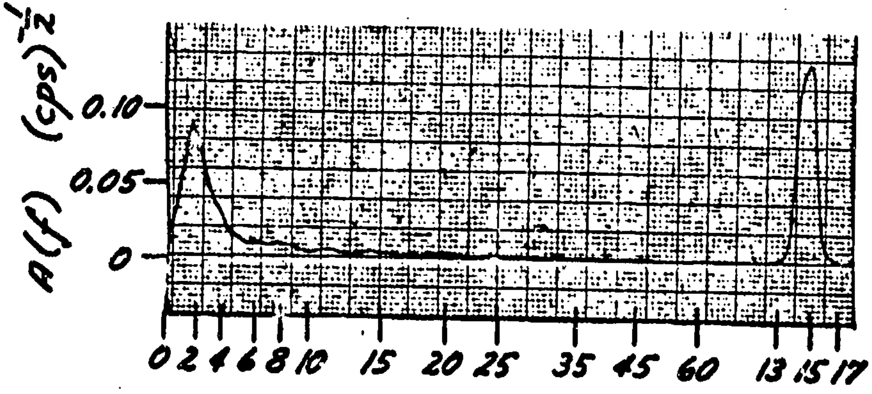

F-80 WITH WING TANKS
3/1/50 RUN 5
1250 Mc/S
AZIMUTH 88°-91°
ELEVATION 6°-6°
RANGE 10,800-10,800 YDS.

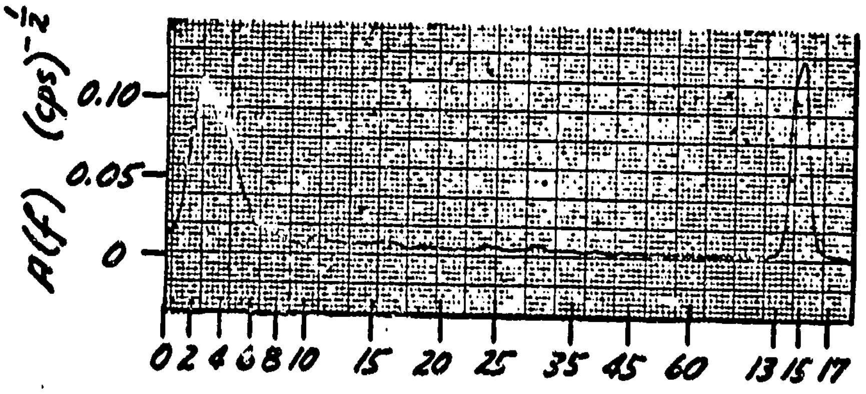

F-80 WITH WING TANKS
3/1/50 RUN 5
2810 Mc/S
AZIMUTH 88°-91°
ELEVATION 6°-6°
RANGE 10,800-10,800 YDS.

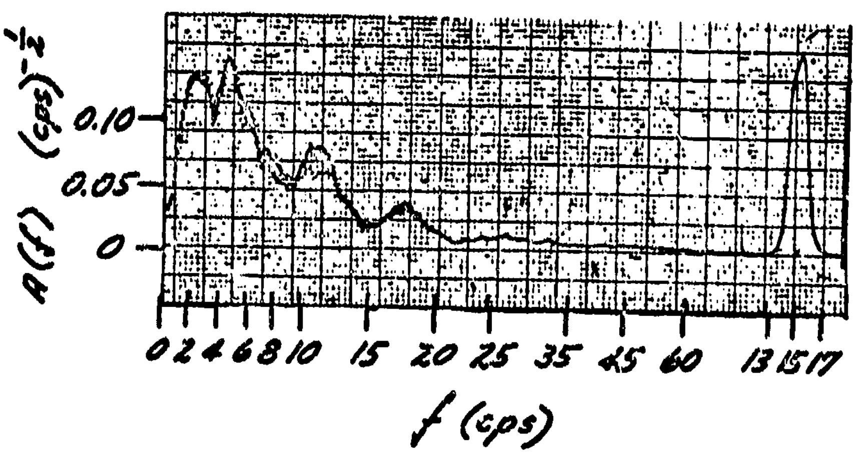

F-80 WITH WING TANKS
3/1/50 RUN 5
9380 Mc/S
AZIMUTH 88°-91°
ELEVATION 6°-6°
RANGE 10,800-10,800 YDS.

Figure 29

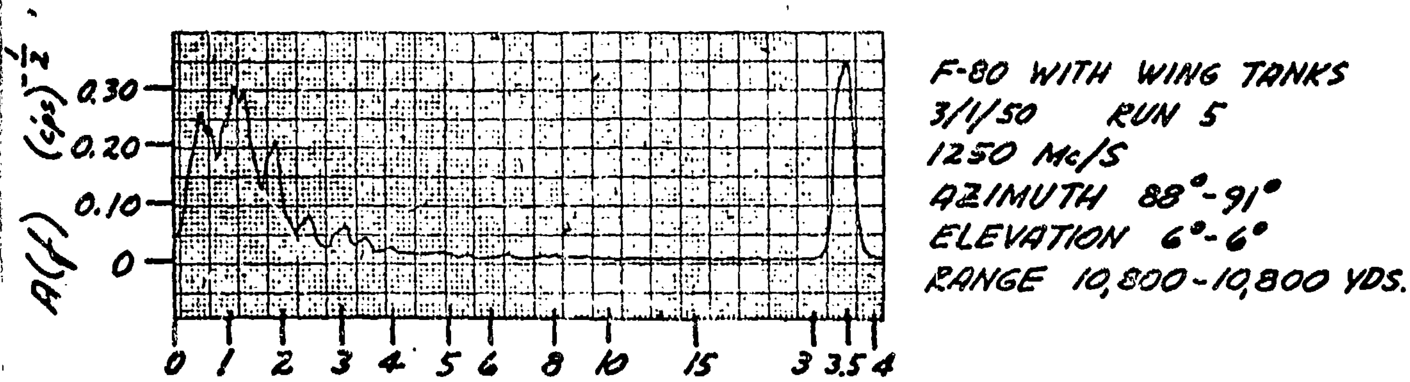
$A(f)\ (cps)^{-\frac{1}{2}}$
0.30
0.20
0.10
0
0 1 2 3 4 5 6 8 10 15 3 3.5 4
F-80 WITH WING TANKS
3/1/50 RUN 5
1250 Mc/S
AZIMUTH 88°-91°
ELEVATION 6°-6°
RANGE 10,800-10,800 YDS.

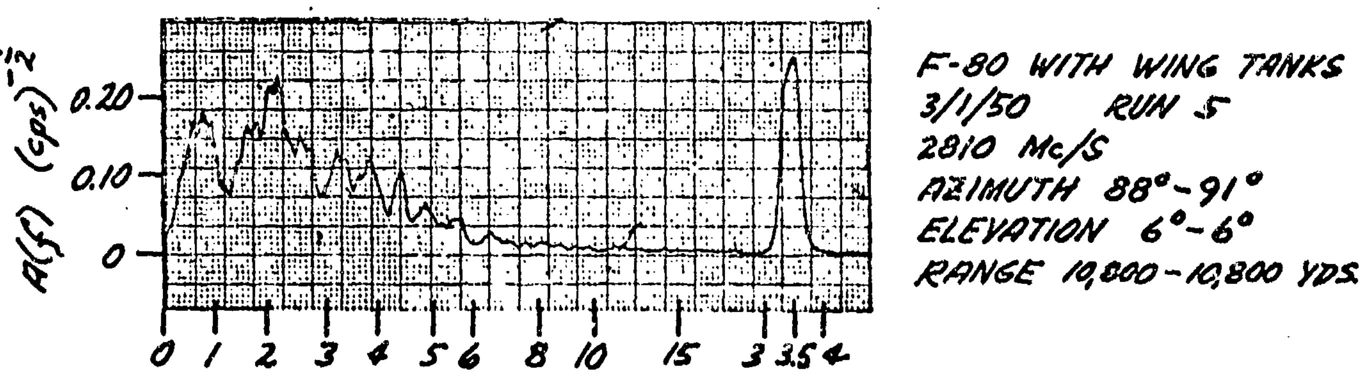
$A(f)\ (cps)^{-\frac{1}{2}}$
0.20
0.10
0
0 1 2 3 4 5 6 8 10 15 3 3.5 4
F-80 WITH WING TANKS
3/1/50 RUN 5
2810 Mc/S
AZIMUTH 88°-91°
ELEVATION 6°-6°
RANGE 10,800-10,800 YDS.

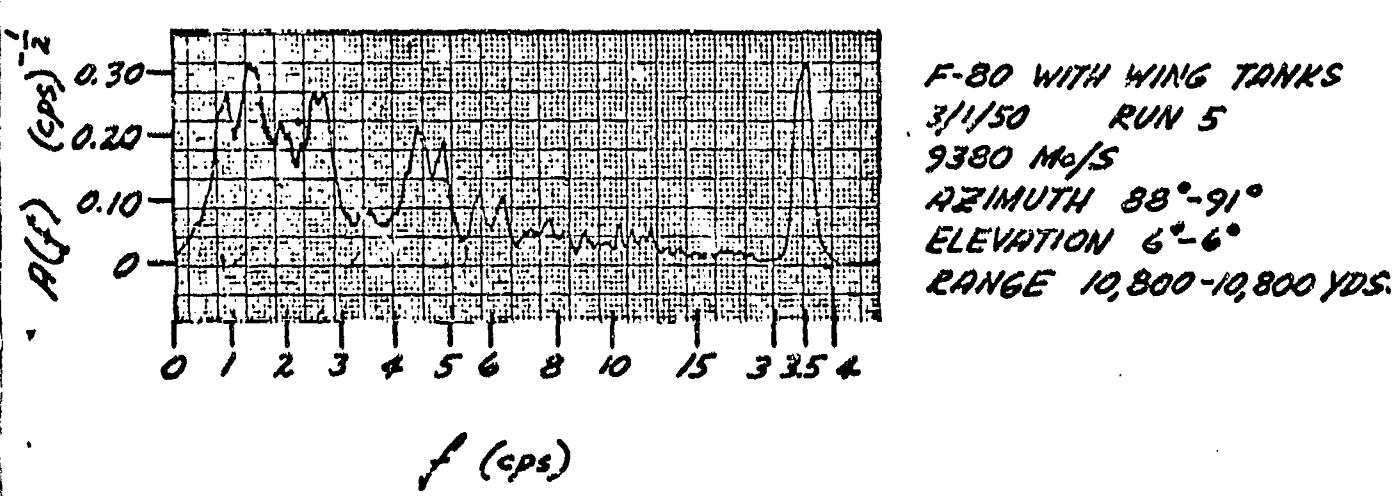
$A(f)\ (cps)^{-\frac{1}{2}}$
0.30
0.20
0.10
0
0 1 2 3 4 5 6 8 10 15 3 3.5 4
f (cps)
F-80 WITH WING TANKS
3/1/50 RUN 5
9380 Mc/S
AZIMUTH 88°-91°
ELEVATION 6°-6°
RANGE 10,800-10,800 YDS.

Figure 30

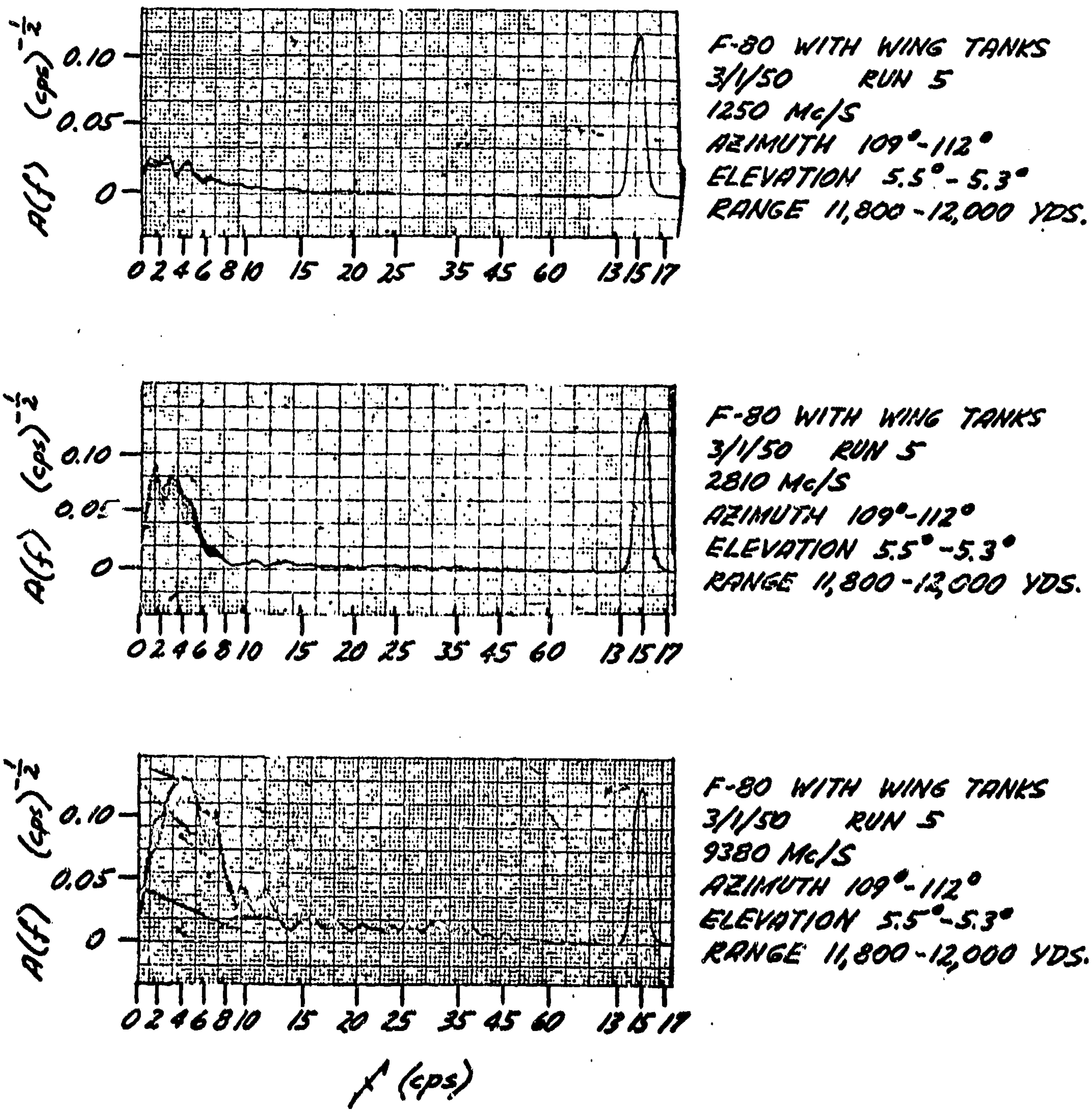
F-80 WITH WING TANKS
3/1/50 RUN 5
1250 Mc/S
AZIMUTH 109°-112°
ELEVATION 5.5°-5.3°
RANGE 11,800-12,000 YDS.
F-80 WITH WING TANKS
3/1/50 RUN 5
2810 Mc/S
AZIMUTH 109°-112°
ELEVATION 5.5°-5.3°
RANGE 11,800-12,000 YDS.
F-80 WITH WING TANKS
3/1/50 RUN 5
9380 Mc/S
AZIMUTH 109°-112°
ELEVATION 5.5°-5.3°
RANGE 11,800-12,000 YDS.
A(f) (cps)^-1/2
0.10
0.05
0
0 2 4 6 8 10 15 20 25 35 45 60 13 15 17
f (cps)

Figure 31

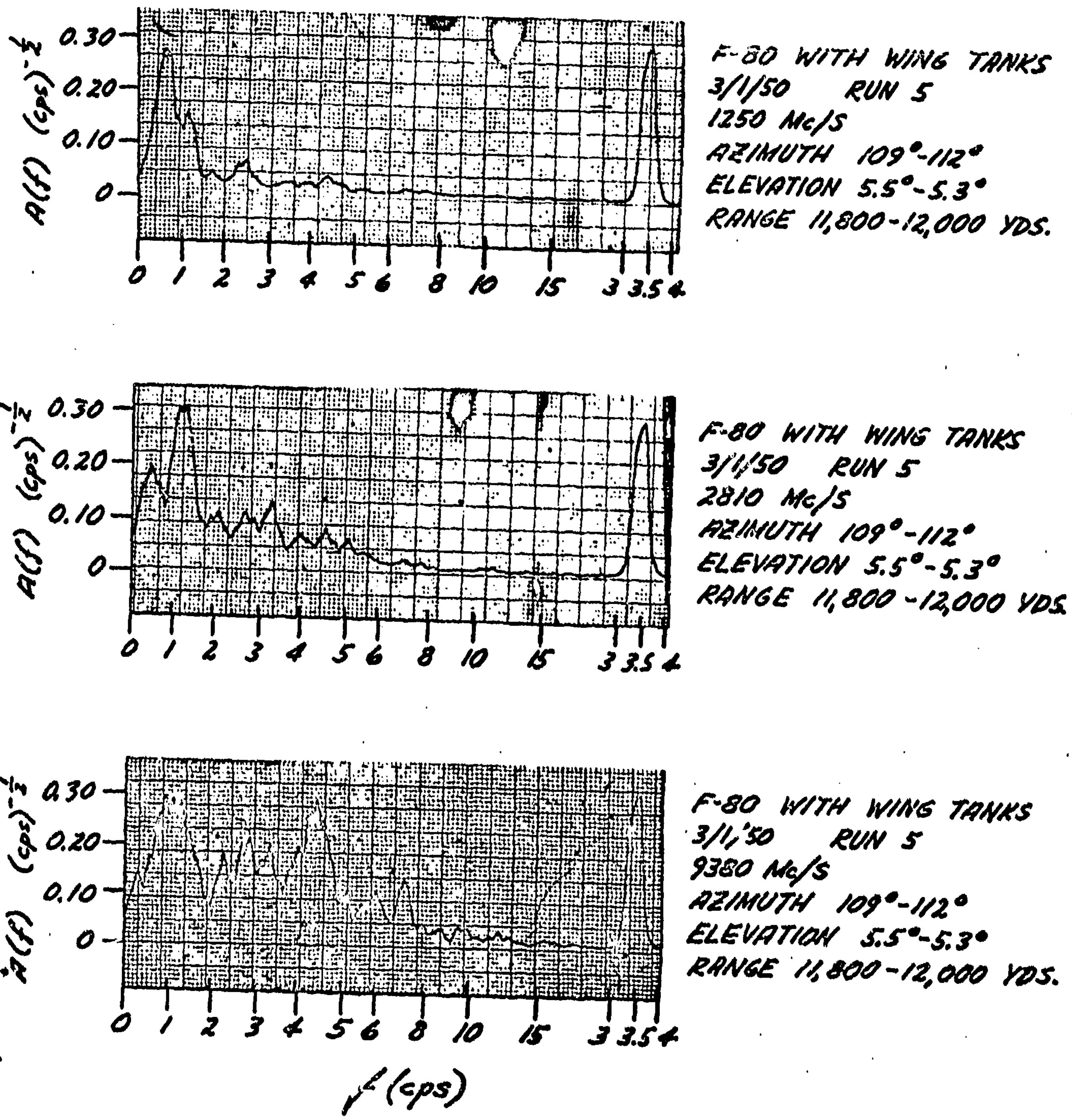
0.30
0.20
0.10
0
A(f) (cps)^-1/2
0 1 2 3 4 5 6 8 10 15 3 3.5 4
F-80 WITH WING TANKS
3/1/50 RUN 5
1250 Mc/S
AZIMUTH 109°-112°
ELEVATION 5.5°-5.3°
RANGE 11,800-12,000 YDS.
F-80 WITH WING TANKS
3/1/50 RUN 5
2810 Mc/S
AZIMUTH 109°-112°
ELEVATION 5.5°-5.3°
RANGE 11,800-12,000 YDS.
F-80 WITH WING TANKS
3/1/50 RUN 5
9380 Mc/S
AZIMUTH 109°-112°
ELEVATION 5.5°-5.3°
RANGE 11,800-12,000 YDS.
f (cps)

Figure 32

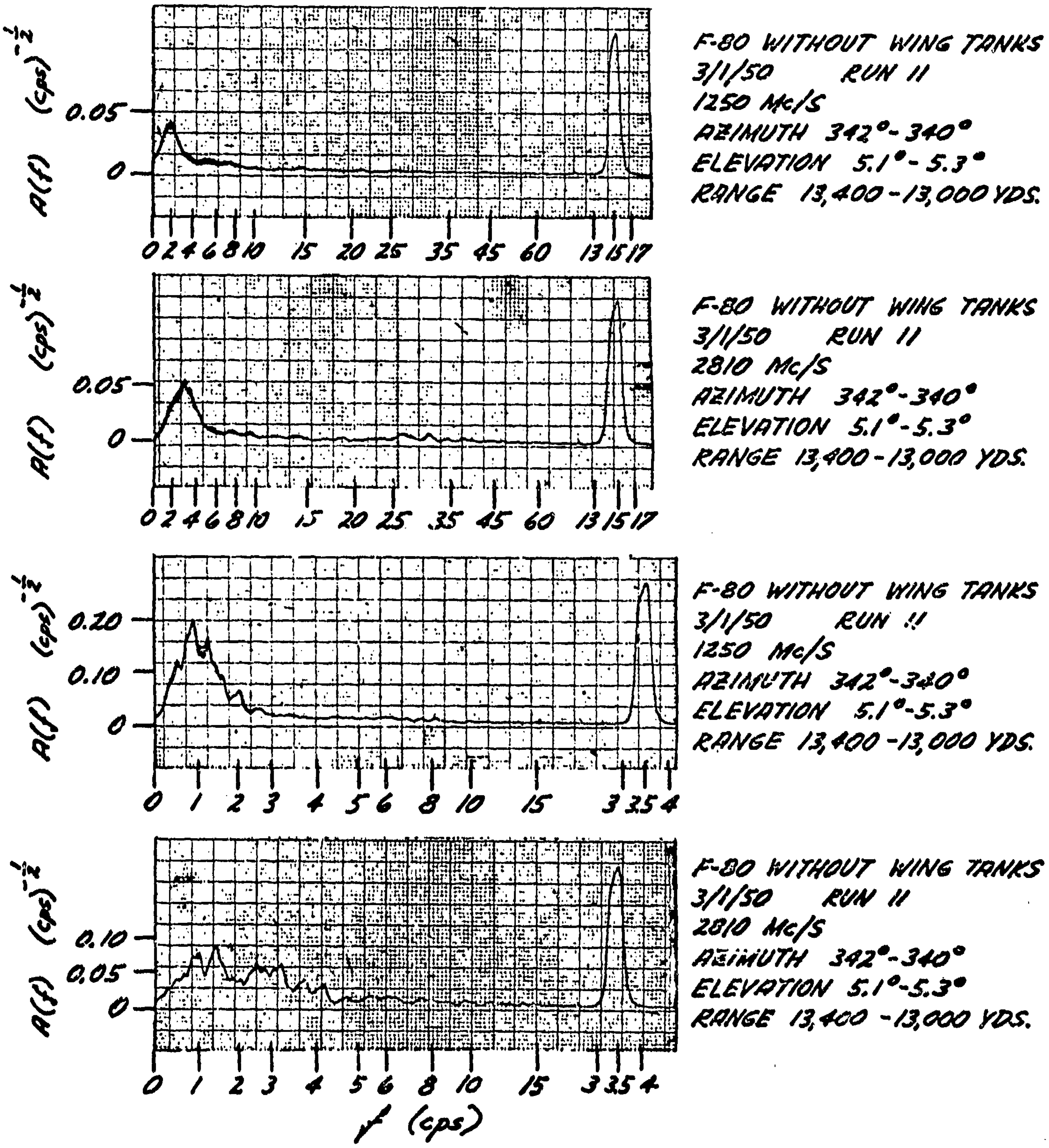
F-80 WITHOUT WING TANKS
3/1/50 RUN 11
1250 Mc/S
AZIMUTH 342°-340°
ELEVATION 5.1°-5.3°
RANGE 13,400-13,000 YDS.
F-80 WITHOUT WING TANKS
3/1/50 RUN 11
2810 Mc/S
AZIMUTH 342°-340°
ELEVATION 5.1°-5.3°
RANGE 13,400-13,000 YDS.
F-80 WITHOUT WING TANKS
3/1/50 RUN 11
1250 Mc/S
AZIMUTH 342°-340°
ELEVATION 5.1°-5.3°
RANGE 13,400-13,000 YDS.
F-80 WITHOUT WING TANKS
3/1/50 RUN 11
2810 Mc/S
AZIMUTH 342°-340°
ELEVATION 5.1°-5.3°
RANGE 13,400-13,000 YDS.
A(f) (cps)^-1/2
0.05
0.20
0.10
0
0 2 4 6 8 10 15 20 25 35 45 60 13 15 17
0 1 2 3 4 5 6 8 10 15 3 3.5 4
f (cps)

Figure 33

[redacted]

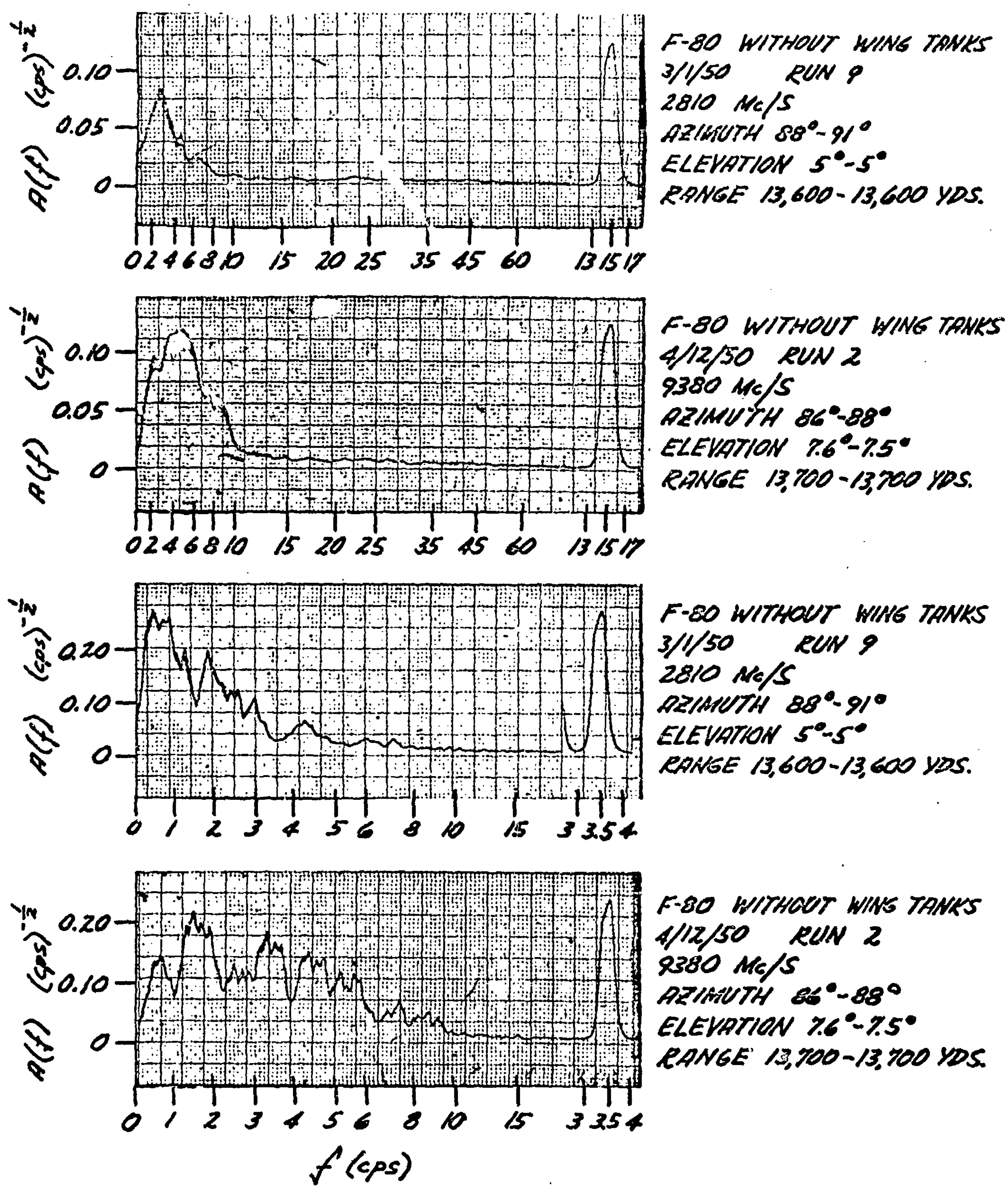

[redacted]

Figure 34

[redacted]

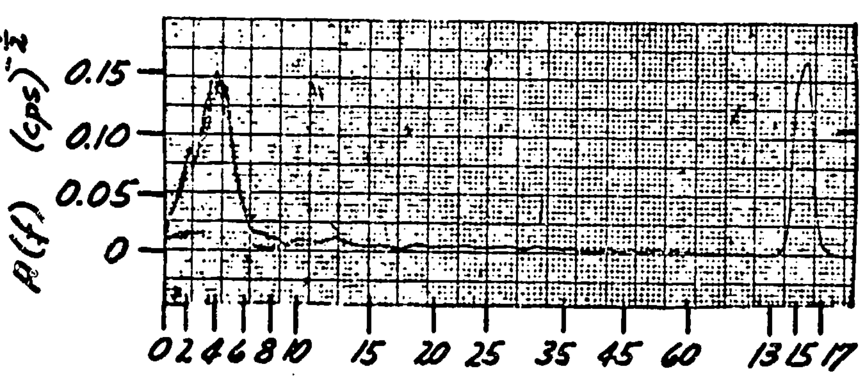

F-80 WITHOUT WING TANKS
3/1/50 RUN 9
2810 Mc/S
AZIMUTH 124°-125°
ELEVATION 4.7°-4.5°
RANGE 17,400-17,700 YDS.

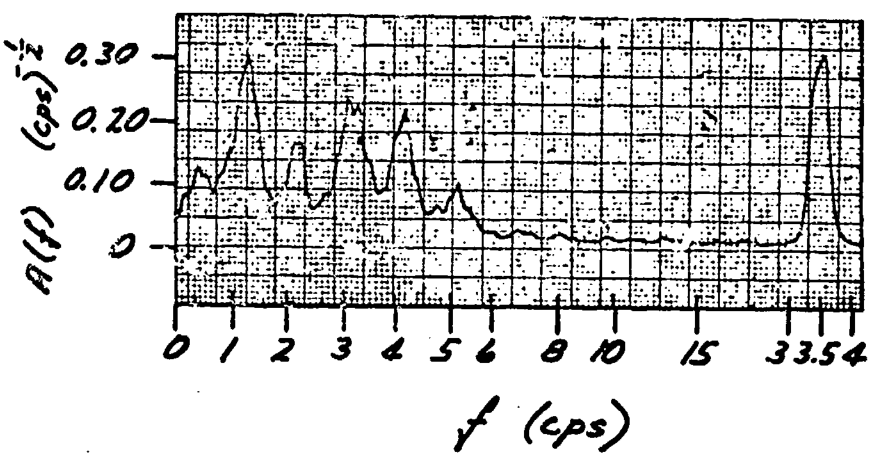

F-80 WITHOUT WING TANKS
3/1/50 RUN 9
2810 Mc/S
AZIMUTH 124°-125°
ELEVATION 4.7°-4.5°
RANGE 17,400-17,700 YDS.

[redacted]

Figure 35